

UNCLASSIFIED

AD NUMBER

ADB018467

LIMITATION CHANGES

TO:

Approved for public release; distribution is unlimited.

FROM:

Distribution authorized to U.S. Gov't. agencies only; Test and Evaluation; APR 1977. Other requests shall be referred to Ballistic Research Lab., Aberdeen Proving Ground, MD.

AUTHORITY

BRL ltr 31 May 1978

THIS PAGE IS UNCLASSIFIED

THIS REPORT HAS BEEN DELIMITED
AND CLEARED FOR PUBLIC RELEASE
UNDER DOD DIRECTIVE 5200.20 AND
NO RESTRICTIONS ARE IMPOSED UPON
ITS USE AND DISCLOSURE.

DISTRIBUTION STATEMENT A

APPROVED FOR PUBLIC RELEASE;
DISTRIBUTION UNLIMITED.

✓
BRL MR 2737

AD B018467

BRL

② 78
AD

MEMORANDUM REPORT NO. 2737

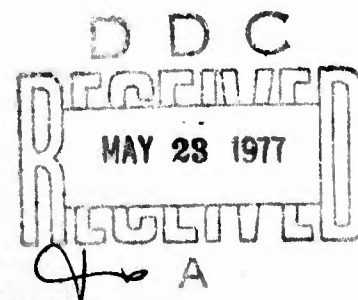
(Supersedes IMR No. 478)

WIND TUNNEL EXPERIMENTS ON THE EFFECT OF
COMBUSTION IN THE WAKE REGION OF
SUPERSONIC PROJECTILES - TEST SERIES III

J. Richard Ward
Frank P. Baltakis
Dennis J. Mancinelli

April 1977

Distribution limited to US Government agencies only; Test and
Evaluation; APR 77. Other requests for this document must be
referred to Director, USA Ballistic Research Laboratory,
ATTN: DRDAR-TSB, Aberdeen Proving Ground, Maryland 21005.



USA ARMAMENT RESEARCH AND DEVELOPMENT COMMAND
USA BALLISTIC RESEARCH LABORATORY ✓
ABERDEEN PROVING GROUND, MARYLAND

AU NO.
DDC FILE COPY

Destroy this report when it is no longer needed.
Do not return it to the originator.

Secondary distribution of this report by originating
or sponsoring activity is prohibited.

Additional copies of this report may be obtained
from the Defense Documentation Center, Cameron
Station, Alexandria, Virginia 22314.

The findings in this report are not to be construed as
an official Department of the Army position, unless
so designated by other authorized documents.

*The use of trade names or manufacturers' names in this report
does not constitute indorsement of any commercial product.*

UNCLASSIFIED

SECURITY CLASSIFICATION OF THIS PAGE (When Data Entered)

REPORT DOCUMENTATION PAGE		READ INSTRUCTIONS BEFORE COMPLETING FORM
1. REPORT NUMBER BRL MEMORANDUM REPORT NO. 2737	2. GOVT ACCESSION NO.	3. RECIPIENT'S CATALOG NUMBER
4. TITLE (and Subtitle) Wind Tunnel Experiments on the Effect of Combustion in the Wake Region of Supersonic Projectiles - Test Series III		5. TYPE OF REPORT & PERIOD COVERED BRL Memorandum Report
6. AUTHOR(s) J. Richard Ward, Frank P. Baltakis Dennis J. Mancinelli		6. PERFORMING ORG. REPORT NUMBER
7. PERFORMING ORGANIZATION NAME AND ADDRESS USA Ballistic Research Laboratory Aberdeen Proving Ground, MD 21005		8. CONTRACT OR GRANT NUMBER(s)
11. CONTROLLING OFFICE NAME AND ADDRESS USA Materiel Development & Readiness Command 5001 Eisenhower Avenue Alexandria, VA 22333		10. PROGRAM ELEMENT, PROJECT, TASK AREA & WORK UNIT NUMBERS 1W662618AH80
14. MONITORING AGENCY NAME & ADDRESS (if different from Controlling Office)		12. REPORT DATE APR 1977
		13. NUMBER OF PAGES 64
		15. SECURITY CLASS. (of this report) Unclassified
16. DISTRIBUTION STATEMENT (of this Report) Distribution limited to US Government agencies only; Test and Evaluation; Apr 1977. Other requests for this document must be referred to Director, USA Ballistic Research Laboratory, ATTN: DRDAR-TSB, Aberdeen Proving Ground, MD 21005.		
17. DISTRIBUTION STATEMENT (of the abstract entered in Block 20, if different from Report)		
18. SUPPLEMENTARY NOTES This report supersedes BRL IMR No. 478, dated February 1976.		
19. KEY WORDS (Continue on reverse side if necessary and identify by block number) base drag; pyrotechnics; tracers; fumers; base bleed; base drag; aerodynamics; extended range.		
20. ABSTRACT (Continue on reverse side if necessary and identify by block number) This report summarizes the third set of wind tunnel tests to evaluate the effect of combustion of pyrotechnics on the base drag of supersonic projectiles. In this test series, a larger diameter model was used to expand the range of injection parameters for R20C. It was found that the base pressure rise vs I, the injection parameter, for R20C could be correlated by an expression requiring two parameters. The maximum base drag reduction achieved with pyrotechnics at $M = 2.0$ was 68%. At sub infinity		

DD FORM 1 JAN 73 1473 EDITION OF 1 NOV 65 IS OBSOLETE

UNCLASSIFIED

SECURITY CLASSIFICATION OF THIS PAGE (When Data Entered)

UNCLASSIFIED

SECURITY CLASSIFICATION OF THIS PAGE(When Data Entered)

The maximum specific impulse at $M_\infty = 2.0$ was nearly 8kN-s/kg. The maximum specific impulse was observed at an I value of 0.002. Direct measurement of the specific impulse by means of a force balance agreed with the specific impulses computed from integrating base pressure-time histories.

UNCLASSIFIED

SECURITY CLASSIFICATION OF THIS PAGE(When Data Entered)

TABLE OF CONTENTS

	<u>Page</u>
LIST OF TABLES	5
LIST OF FIGURES	7
LIST OF SYMBOLS	9
I. INTRODUCTION	11
II. EXPERIMENTAL	11
<u>Test Facility</u>	11
<u>Model and Instrumentation</u>	11
<u>Fumer Mixes</u>	16
III. RESULTS	18
<u>Base Pressure Data</u>	18
<u>Force Balance Measurements</u>	19
IV. DISCUSSION	22
V. CONCLUSIONS	38
REFERENCES	39
APPENDIX A	41
DISTRIBUTION LIST	59

APPROVED FOR	
ADVIS	ADVIS Section <input type="checkbox"/>
ADD	ADD Section <input checked="" type="checkbox"/>
UNCLASSIFIED	UNCLASSIFIED <input type="checkbox"/>
JUSTIFICATION	
BY	
DISTRIBUTION/AVAILABILITY CODES	
Dist.	AVAIL. and/or SPECIAL
B	

LIST OF TABLES

<u>Table</u>		<u>Page</u>
I	Summary of Test Conditions.	14
II	Composition of Standard Fumer Mixes Examined in Wind Tunnel Experiments	18
III	Summary of Test Results for Experiments in Which Combustion Occurred	20
IV	Base Pressure for Tests in Which Combustion of the Fumer Could be Distinguished From the Igniter	22
V	Specific Impulses of Fumer Mixes in Table IV.	29
VI	Comparison Between Specific Impulses Measured by the Force Balance with those Inferred from Pressure Orifices	35
VII	Summary of Results for Various Fuel/Oxidizer Combinations Tested	36
VIII	Base Drag Reductions and Injection Parameters for Smooth-Burning Mixes with No Quantitative Computer Output	37

LIST OF FIGURES

<u>Figure</u>	<u>Page</u>
1 Wind Tunnel Test Setup.	12
2 Pressure Orifice Location and Fumer Capsule	13
3 Diagram of the Fumer Capsule with the Force Balance and with the Spin Mechanism	17
4 Summary of Reid and Hastings' Results with Various Values of d_f/d vs I	24
5 Increase in Base Pressure vs I for R20C	25
6 Increase in Base Pressure vs I for R20C and $\text{NaBH}_4/\text{Sr}(\text{NO}_3)_2$	26
7 Increase in Base Pressure vs I for R20C, $\text{NaBH}_4/$ $\text{Sr}(\text{NO}_3)_2$, and AP-Mix.	28
8 Specific Impulse vs I for Fumer Mixes from Table IV, $M_\infty=2.0$	30
9 Increase in Base Pressure vs I	32
10 Increase in Base Pressure vs I with Eq. (10).	34

LIST OF SYMBOLS

A	area of the base of the wind tunnel model
C_{Db}	base drag coefficient
ΔC_{Db}	change in C_{Db} due to combustion
df	diameter of the fumer cavity
d	diameter of the wind tunnel model
I	injection parameter
Isp	specific impulse
J	constant used in the correlation of base drag reduction and the injection parameter
l	length of burning column
M	Mach number
m	mass
\dot{m}	mass burning rate
P	pressure
P_b	base pressure
P1...P8	pressure tap designation
ΔP_b	change in base pressure due to combustion
$\Delta(P_b/P_\infty)$	change in the ratio of base pressure to free-stream pressure due to combustion
ρ	density
r	linear burning rate
U	air speed
T	temperature
tb	burning time

Subscripts

i	initial conditions
c	during combustion
f	fumer mix
ig	igniter mix
∞	free-stream conditions
o	stagnation conditions

I. INTRODUCTION

This report summarizes the results from the third set of wind tunnel tests to evaluate how effectively pyrotechnics reduce projectile base drag. Previous experiments^{1,2} concentrated on pyrotechnic formulations similar to those used in tracer rounds, since such formulations were expected to ignite and burn at subatmospheric pressure. The main objective of the present tests was to examine a variety of fuels and oxidizers as potential fumer mixes. In addition, some earlier experiments were repeated with a 64mm diameter model in place of the standard 25mm diameter model. Tests were also made with a force balance to compare specific impulses computed from pressure measurements with specific impulses measured directly with the force balance.

II. EXPERIMENTAL

Test Facility

The experiments were conducted in a wind tunnel at Mach 2 at duplicated sea-level pressure and temperature conditions. The facility used was the Naval Surface Weapons Center's Hypersonic Tunnel which has a large capacity air supply and heating system. Normally, this tunnel is operated at Mach numbers 5 to 10. Recently it has been equipped with two additional stilling chambers which permit its operation at supersonic Mach numbers at duplicated sea-level temperature and pressure conditions. The flow nozzles used in this study were of centerbody-type design, 15 or 30cm exit diameter and were procured specifically for projectile base flow studies. The overall tunnel system and the new stilling chamber were depicted previously.^{1,2} The test setup is illustrated on Figure 1. Wind tunnel conditions for each test run are given in Table I.

Model and Instrumentation

Projectile base flow was simulated using a bluff cylindrical model which was supported in the stilling chamber and extended through the nozzle throat into the test section (Figure 2). Two sizes, 25 and 64mm diameter models were used. Model lengths, measured from the nozzle throat, were 26.7cm and 46cm for the 25mm and 64mm diameter models, respectively.

Both models were equipped with air turbines capable of spin rates of up to 50 krpm and with force balances for direct base drag measurements (Figure 3). Pressure orifices were provided near the model periphery for base drag determination during tests with spin.

¹ J. R. Ward, F. P. Baltakis, S. W. Pronchick, "Wind Tunnel Study of Base Drag Reduction by Combustion of Pyrotechnics," BRL Report No. 1745, October 1974, (AD #B000431L).

² J. R. Ward, F. P. Baltakis, D. Mancinelli, and T. Elmendorf, "Wind Tunnel Experiments on the Effect of Combustion in the Wake Region of Supersonic Projectiles," BRL Memorandum Report No. 2588, February 1976, (AD #B009982L).

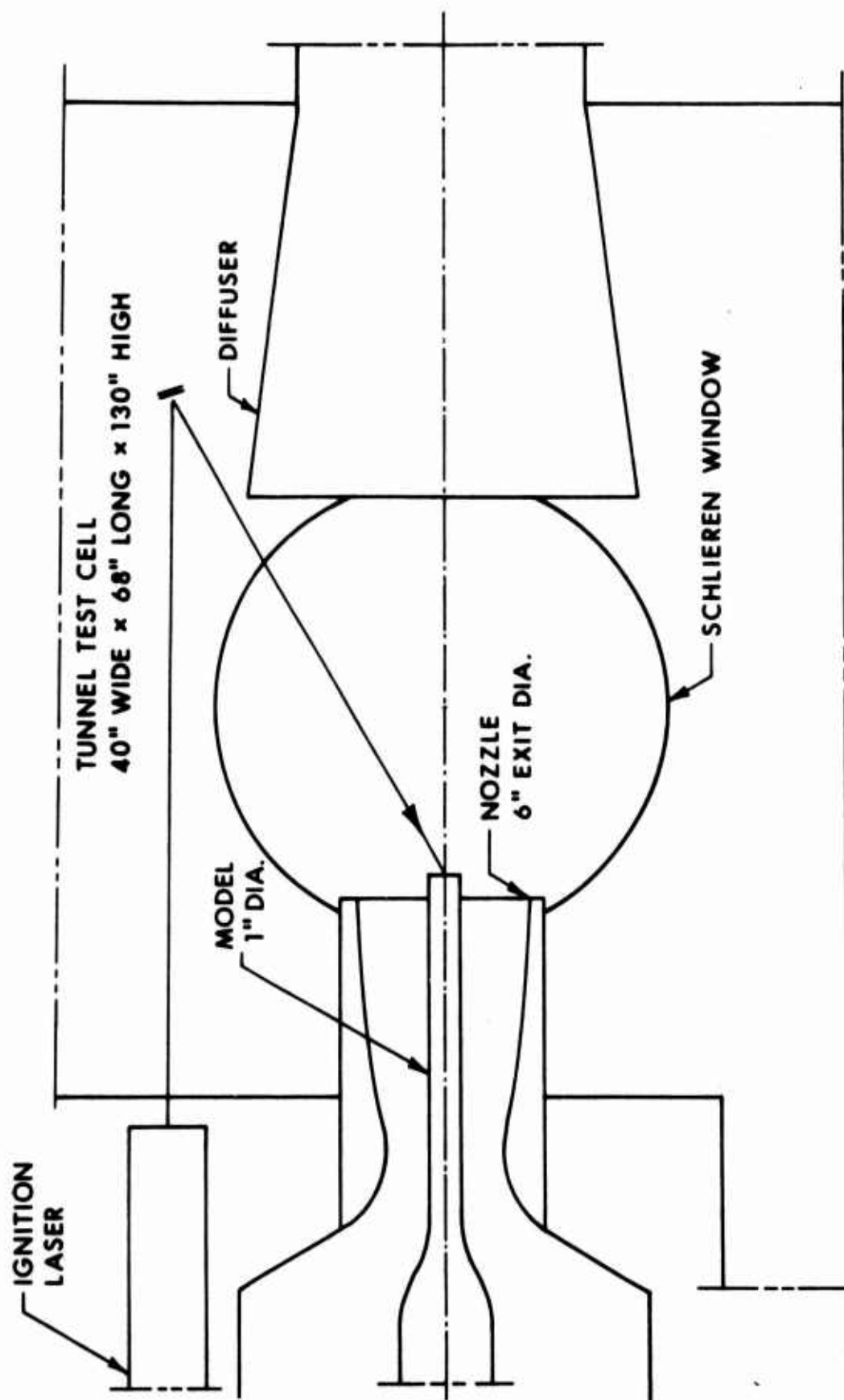


Figure 1. Wind Tunnel Test Setup

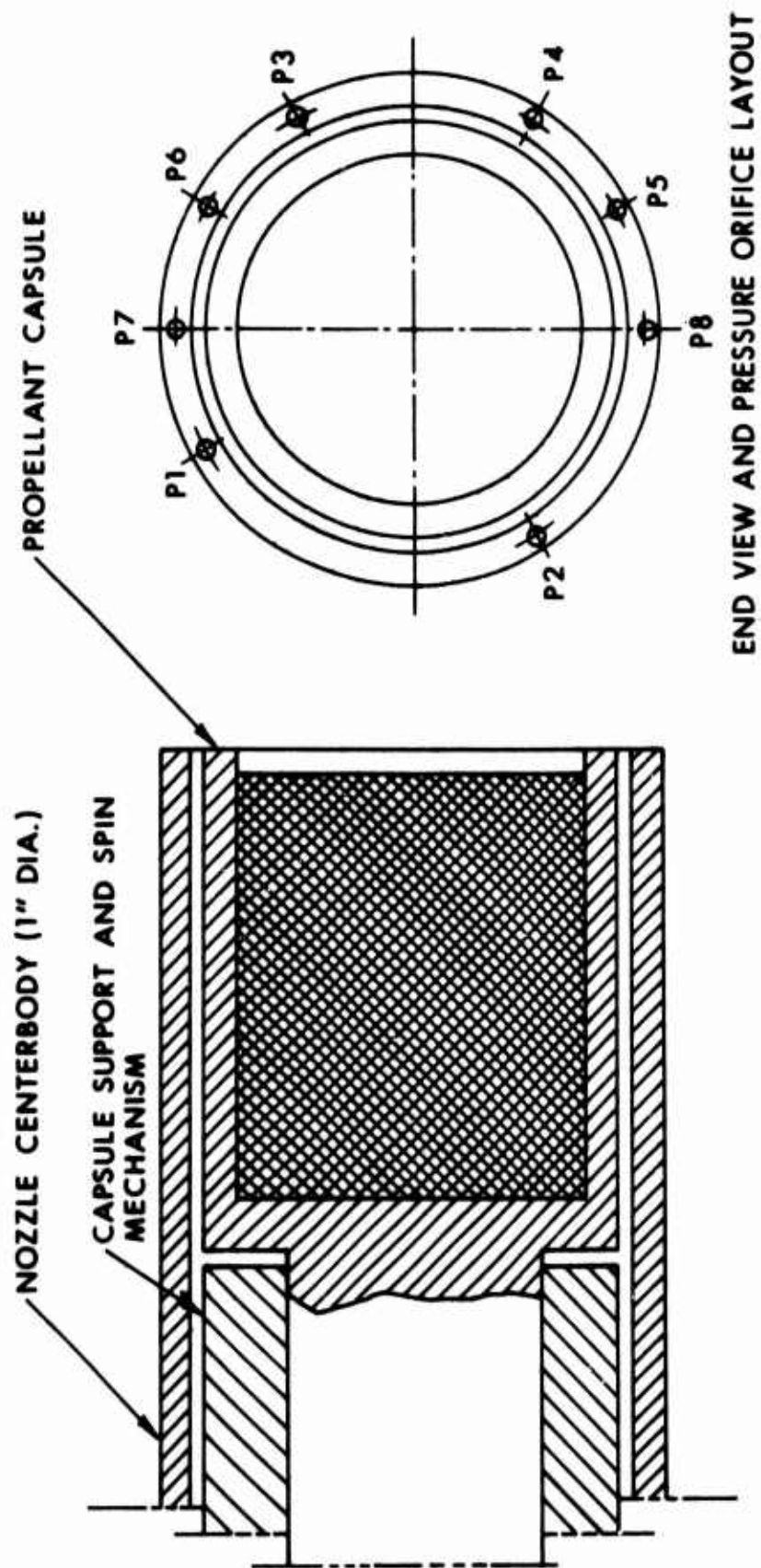


Figure 2. Pressure Orifice Location and Fumer Capsule

TABLE I. Summary of Test Conditions

Run	M_∞	P_o , bar	T_o , K	Fumer Composition, Percent by Weight	Remarks
18	1.97	6.4	483	R20C	64mm diameter model
19	1.97	6.5	489	R20C	64mm diameter model
49	1.97	6.6	486	R20C	64mm diameter model, spinning at 18 krpm.
51	1.97	6.9	489	R20C	Force balance test
52	1.97	6.8	492	R20C	Force balance test
53	1.97	6.9	492	R20C	Force balance test
54	1.99	6.8	492	NaBH ₄ /Sr(NO ₃) ₂ , 40/60	
56	1.99	6.8	472	NaBH ₄ /Sr(NO ₃) ₂ , 15/85	
57	1.99	7.0	484	NaBH ₄ /Sr(NO ₃) ₂ , 25/75	
58	1.99	7.1	489	NaBH ₄ /Sr(NO ₃) ₂ , 35/65	
59	1.99	6.7	489	ZrH ₂ /Sr(NO ₃) ₂ , 70/30	No ignition
60	1.99	7.0	492	Zr/H ₂ /Sr(NO ₃) ₂ , 50/50	No ignition
61	1.99	6.8	489	MgH ₂ /Sr(NO ₃) ₂ , 24/76	No ignition
62	1.99	7.0	494	Mg/SrO ₂ /oxamide, 14/81/5	No ignition
63	1.99	6.9	492	F-4/azocel, 90/10	Delayed ignition
64	1.99	6.7	494	F-4/azocel, 90/10	Delayed ignition
65	1.99	6.9	494	F-4	Delayed ignition
66	1.99	7.0	494	E-B ^a	
67	1.99	7.0	494	E-B ^a	
68	1.99	6.9	494	NaBH ₄ /Sr(NO ₃) ₂ , 25/75	
69	1.99	6.9	494	NaBH ₄ /Sr(NO ₃) ₂ , 35/65	

Table I (Continued)

Run	M_∞	P_0 , bar	T_0 , K	Fumer Composition, Percent by Weight	Remarks
70	1.99	6.9	494	B/BaCrO ₄ , 15/85	No ignition
71	1.99	6.9	494	B/KClO ₄ , 31/69	
72	1.99	6.9	494	Mg/SrO ₂ /C.R. ^b , 15/83/2	No ignition
73	1.99	6.9	494	Zr/Sr(NO ₃) ₂ /C.R., 47/43/10	
74	1.99	6.9	494	Zr/KClO ₄ , 57/43	
75	1.99	6.9	494	Zr/KClO ₄ /C.R., 51/39/10	No ignition
76	1.99	6.9	494	Ti/KClO ₄ , 33/67	No ignition
77	1.99	6.9	494	Mg/KClO ₄ /C.R., 37/53/10	
78	1.99	6.9	494	Zr/Sr(NO ₃) ₂ , 52/48	
79	1.99	6.9	494	Repeat Run 78	Delayed ignition
80	1.99	6.9	494	Ti/Sr(NO ₃) ₂ , 36/64	No ignition
81	1.99	6.9	494	Ti/Sr(NO ₃) ₂ /CR, 32/58/10	
82	1.99	6.9	494	F-4/RDX, 96/4	Delayed ignition
83	1.99	6.9	494	NaBH ₄ /Sr(NO ₃) ₂ , 40/60	
84	1.99	6.9	494	ZrH ₂ /Sr(NO ₃) ₂ , 50/50	No ignition
85	1.99	6.9	494	F-4/HES ^c , 90/10	
86	1.99	6.9	494	Ti/KClO ₄ /CR, 30/60/10	
87	1.99	6.9	494	F-4, 149-250 μ Mg	
88	1.99	6.9	494	F-4/TNT, 96/4	
89	1.99	6.9	494	Ti/Sr(NO ₃) ₂ , 36/64	

Table I (Continued)					
Run	M_{∞}	P_0 , bar	T_0 , K	Fumer Composition, Percent by Weight	Remarks
90	1.99	6.9	494	Ti, $KClO_4$, 33,67	No ignition
91	1.99	6.9	494	F-4, 74-100 μ Mg	
92	1.99	6.9	494	F-4, 44-100 μ Mg	
93	1.99	6.9	494	F-4, <44 μ Mg	
94	1.99	6.9	494	B/ $KClO_4$, 31/69	
95	1.99	6.9	494	Mg/ SrO_2 /CR, 15,83,2	No ignition

^a Proprietary mix from the Ensign-Bickford Co. Approximate composition in percent by weight

Mg(25 \pm 5), $Sr(NO_3)_2$ (35 \pm 5), PVC (10), DOP (10), AP(20) where

PVC is polyvinylchloride,
DOP is dioctylphthalate,
AP is ammonium perchlorate.

^b Calcium resinate.

^c Propellant supplied by Hercules Co. No analysis given.

The propellant for each run was contained in a separate steel capsule and was ignited with a laser light beam. A 250-watt CO_2 gas laser was used and arranged as shown on Figure 1. The light beam diameter at the plane of impingement was about one cm and the exposure time ranged from two to five seconds.

Fumer Mixes

The fumer mixes were charged at a pressure of 282 MN/m² (40,900 psi) at the Frankford Arsenal's Pyrotechnics Laboratory. The pressure was calibrated with a Webster force gage. A layer of R20C mix was pressed onto each fumer mix to assist in the ignition of the mix. With the exception of experiments with fumer mixes R20C and F-4, the fumer mix consisted of a fuel and oxidizer or a fuel, oxidizer, and one burning rate modifier. The chemical composition of R20C and F-4 is included in Table II.

The mass and the column height of each fumer mix and igniter mix were also measured in order to calculate mass burning rates.

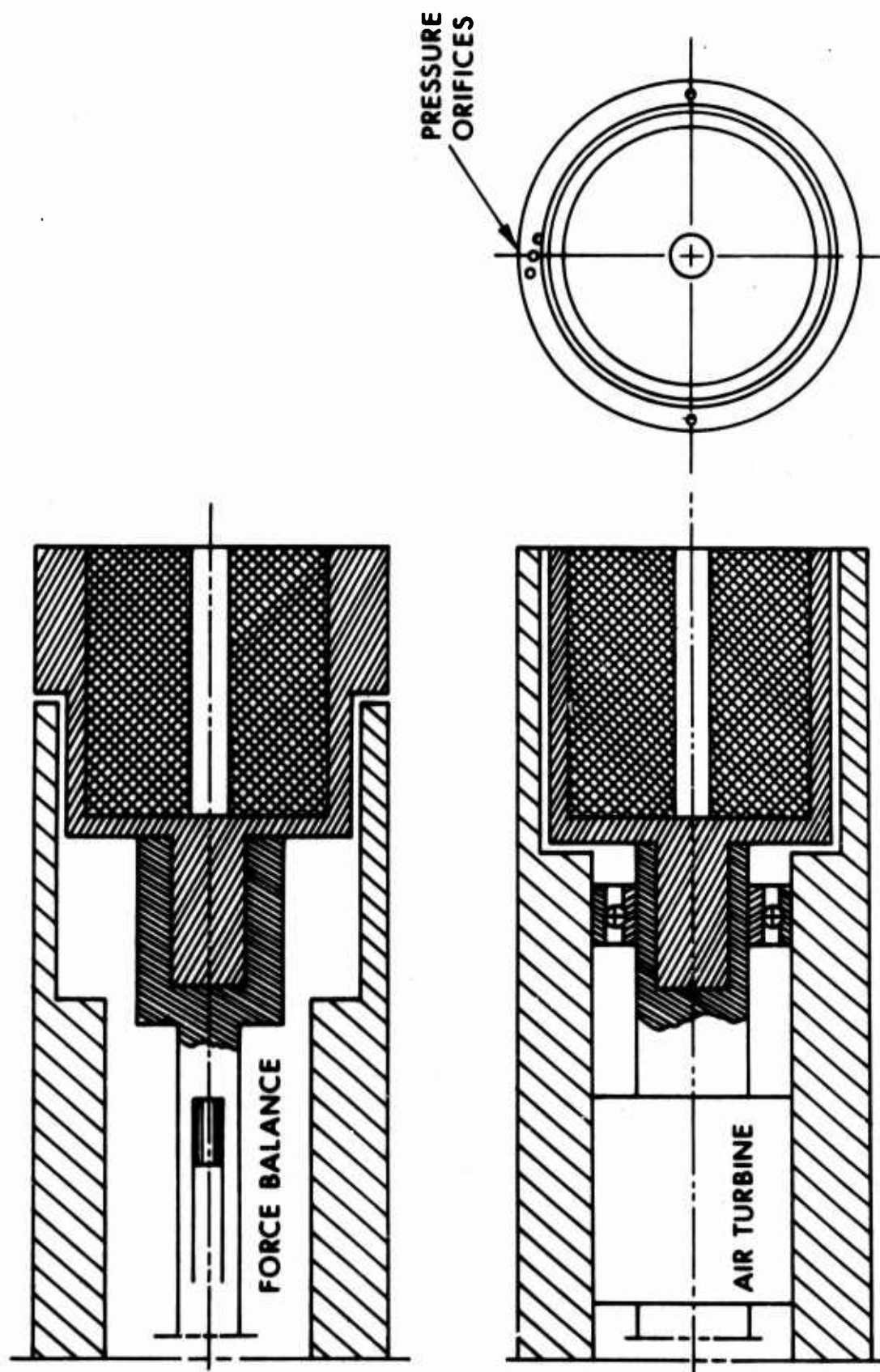


Figure 3. Diagram of the Fumer Capsule with the Force Balance and with the Spin Mechanism

Table II. Composition of Standard Fumer Mixes
Examined in Wind Tunnel Experiments

<u>Designation</u>	<u>Constituents, percent by weight</u>	
R20C	Mg, grade 12 ^a ,	21.5
	SrO ₂	65.7
	PbO ₂	3.4
	BaO ₂	3.4
	C.R. ^b	6.0
F-1	Mg, grade 11 ^a	8.1
	SrO ₂	78.8
	C	4.0
	C.R. ^b	9.1
F-4	Mg, grade 11 ^a	33.2
	Sr(NO ₃) ₂ ,	57.7
	C.R. ^b	9.1
R284	Mg, grade 11 ^a	28.0
	Sr(NO ₃) ₂	55.0
	C.R. ^b	17.0

^aMagnesium specification as given in Mil Spec JAN-M-382A.

^bCalcium resinate.

III. RESULTS

Base Pressure Data

The performance parameters of primary interest in this work are base pressure increase and the fumer specific impulse. The base pressure increase was recorded directly versus time. The specific impulse was obtained by integrating the base pressure increase with respect to time and then multiplying by the ratio of A/m_f .

The base pressure increase was found to vary considerably with time. Mixes which ignited quickly generally yielded a step-type pressure pulse. Those mixes which ignited more slowly yielded gradual pressure increases.

Pressure-time histories for test runs which ignited are shown in the Appendix. The time is shown in seconds and the base pressure is normalized to the free-stream static pressure. For a number of runs only qualitative variation is shown. During these runs, due to malfunctioning of the data recording system, pressure data were recorded

using an auxiliary printing system and quantitative computer plotting was not available.

It may be noted on many runs that the main pressure rise is preceded by a sharp spike corresponding to the combustion of the igniter mix (R20C). In some runs the base pressure at the end of burning is higher than the pre-combustion value. Presumably this is from formation of slag on the face of the wind tunnel model that obstructed the pressure taps.

The reduction of the base drag coefficient during combustion is

$$\frac{\Delta C_{Db}}{C_{Db}} = \frac{\Delta P_b}{P_\infty - P_{b_i}} \quad (1)$$

For those tests in which the fumer mix ignited rapidly and burned evenly to yield step-like pressure-time histories, ΔP_b was constant over the run and the mass burning rate of the fumer mix could be inferred. For the tests which did not yield step-like pressure-time histories, the following expression was devised to estimate an average ΔP_b ,

$$\Delta P_b = (tb)^{-1} \int_0^{tb} [(P_b)_t - (P_b)_i] dt \quad (2)$$

where P_{bt} is the base pressure at time t ,

tb = time during which the base pressure is at least 25% greater than $(P_b)_i$.

For the majority of tests, the specific impulse was based on pressure data taken at orifice P3 (Figure 2). For some tests data from other pressure orifices were used. In most cases the agreement between the specific impulse values computed from data at different pressure taps was well within ± 10 percent.

The injection parameter was computed from

$$I = \frac{\dot{m}}{\rho_\infty U_\infty A} \quad (3)$$

Force Balance Measurements

Direct measurements of the reduction in drag force by combustion were attempted with both the 25mm and 64mm diameter models. The force balance was designed originally for use with the 25mm diameter model. In the 64mm diameter model, the force balance was overloaded (Runs 11-17).

The force measurements were made with R20C, since this mix ignited easily and yielded step-like base pressure-time histories. All results pertinent to subsequent discussion are presented in Table III.

TABLE III. Summary of Test Results for Experiments in which Combustion Occurred

Run	m_f, g	m_{ig}, g	l_f, mm	l_{ig}, mm	$\rho_f, g/cm^3$	tb, s	$I \times 10^3$	ΔC_{Db}	Isp, N-s/g ^a
18	11.1	-	18.9	-	2.36	4.1	0.90	0.23	6.8 5.6(P1)
19	11.1	-	18.2	-	2.46	3.6	1.0	0.26	7.1 6.6(P1)
49	11.1	-	18.0	-	2.48	1.2	3.1	0.29	- 4.4(P6)
51	10.6	-	18.3	-	2.34	3.4	8.8	-	3.2, force ^b
52	10.6	-	18.3	-	2.34	3.2	9.7	-	3.1, force ^b
53	10.5	-	17.9	-	2.36	3.2	8.8	-	2.5, force ^b
54	7.7	0.8	18.9	1.1	1.64	3.1	7.3	0.45	2.8 2.6(P2)
56	9.4	0.8	18.0	1.2	2.11	2.4	11.0	0.47	1.8 1.6(P2)
57	8.7	0.9	18.6	1.1	1.89	2.9	8.8	0.51	2.6 2.1(P2)
58	8.2	0.9	19.4	1.1	1.70	4.5	5.4	0.45	3.7 -
63	8.9	1.1	19.0	1.4	1.88	7.7	3.5	0.40	4.9 -
64	9.0	1.0	19.0	1.3	1.91	9.8	2.7	0.33	5.2 -
65	9.7	0.9	17.7	1.4	2.21	8.7	3.5	0.33	4.4 3.9(P2)
66	7.8	0.8	19.5	1.0	1.61	11.2	2.0	0.40	8.5 7.5(P2)
67	8.1	0.7	19.8	1.0	1.65	11.3	2.1	0.39	8.0 6.7(P2)
68	9.0	1.0	19.0	1.1	1.91	2.5	11.0	0.45	- 1.5(P1)
69	8.1	0.9	19.5	1.1	1.67	5.0	4.8	0.48	- 2.9(P1)
71	7.2	1.3	14.8	2.8	1.96	2.6	8.7	0.48	2.1 -
73	12.8	0.8	18.3	1.1	2.82	11.4	3.2	0.32	3.9 -
74	14.1	0.9	18.9	1.2	3.00	2.1	19.0	0.59	1.2 -

Table III (Continued)

Run	m_f, g	m_{ig}, g	l_f, mm	l_{ig}, mm	$\rho_f, g/cm^3$	tb, s	$I \times 10^3$	ΔC_{Db}	Isp, N-s/g ^a
77	8.0	0.8	18.0	1.1	1.80	13.4	1.8	0.31	7.0 -
78	14.7	0.8	17.8	1.0	3.32	2.2	19.0	0.49	1.0 -
79	8.2	0.8	18.0	1.2	1.84	8.7	2.8	0.46	6.4 -
81	11.6	0.6	18.4	0.94	2.54	2.7	12.0	0.57	1.8 -
82	8.2	0.9	17.8	1.3	1.86	8.7	2.8	0.38	5.4 -
83	7.9	0.6	19.3	0.4	1.65	4.4	5.1	0.51	3.9 -
85	8.4	0.8	18.1	1.1	1.87	11.6	2.1	0.33	5.8 -
86	10.2	0.6	18.7	0.6	2.20	18.1	1.6	0.20	4.8 -
87	8.2	1.0	17.8	1.3	1.86	13.4	1.8	0.26	5.5 -
88	8.4	0.8	17.1	1.2	1.98	6.8	3.7	0.40	4.2 -
89	11.2	0.7	17.9	0.9	2.53	17.0	1.9	0.20	4.3 -
91	7.9	1.0	17.1	1.4	1.86	8.6	2.8	0.38	5.4 4.5(P1)
92	7.9	0.9	16.6	1.4	1.91	8.1	2.9	0.39	5.2 4.6(P1)
93	7.8	0.8	16.4	1.2	1.92	7.1	9.4	0.46	5.7 4.5(P1)
94	6.1	1.4	13.4	1.5	1.84	2.4	8.5	0.49	2.3 -

^a First entry is Isp measured from P3. Second entry is Isp measured from pressure orifice indicated.

^b Isp from force balance measurement.

IV. DISCUSSION

In the previous wind tunnel tests,² it was shown that the base pressure increase due to combustion of the pyrotechnic could be correlated to the injection parameter. One objective of the present test series was to see if alternate fuels and oxidizers obeyed the same trend, or perhaps some combination would be superior to the base drag reductions observed to date. To properly compare the present tests with those in reference 2, one must separate the effect of the igniter mix on base pressure from the effect of the fumer mix. This can be done only if quantitative computer plots of base pressure vs time are available. Furthermore, it is necessary that the fumer mix have a constant mass burning rate in order to compute the injection parameter. Table IV lists the runs that satisfy these two criteria.

Table IV. Base Pressure for Tests in Which Combustion of the Fumer Could be Distinguished From the Igniter

Run	\dot{m}_f , g	t_b , s	\dot{m}_f , g/s	$I \times 10^3$	$(P_b/P_\infty)_i$	$\Delta(P_b/P_\infty)$	% C_{Db} reduced
18	11.1	3.8	2.9	0.97	0.68 ^a	0.067	21
19	11.1	3.6	3.1	1.0	0.68 ^a	0.085	27
49	11.1	1.1	10.0	3.4	0.67 ^{a,b}	0.16	48
56	9.4	1.4	6.7	18.0	0.62	0.26	68
57	8.7	1.8	4.8	13.0	0.62	0.23	60
66	7.8	9.4	0.83	2.2	0.62	0.16	42
67	8.1	9.3	0.87	2.4	0.62	0.17	45

^a 64mm diameter model.

^b Spin rate 18 krpm.

Runs 18, 19, and 49 were made with the 64mm diameter model. The object of these tests was to obtain base pressure measurements for R20C at lower values of I than could be obtained with the standard 25mm diameter model used in all the previous tests. Previous wind tunnel experiments with cold gases^{3,4} and with pyrotechnics² demonstrated

³ J. Reid and R. C. Hastings, "The Effect of a Central Jet on the Base Pressure of a Cylindrical Afterbody in a Supersonic Stream," RAE Report No. Aero. 2621, 1959.

⁴ L. D. Kayser, "Effects of Base Bleed and Supersonic Nozzle Injection on Base Pressure," BRL Memorandum Report No. 2456, March 1975, (AD #B003442L).

that the base pressure increase for a given value of I is independent of d_f/d for I less than 0.005. Such results for gases injected into the wake are illustrated in Figure 4. As indicated in Table IV, the 64mm diameter model provides data for I values of 0.001 and 0.0034, within the region of I where the base pressure rise is independent of d_f/d .

In Figure 5 the base pressure increase is plotted as a function of I for all runs in the three wind tunnel test series with R20C. From Figure 5, it is evident that a maximum base pressure increase has been reached with values of I greater than 0.02, and that a sizeable increase in base pressure results for injection values below 0.005. The general trend of base pressure vs I exhibited in Figure 5 is similar to the trend for the injection of gases as in Figure 4.

Runs 56 and 57 were made with NaBH_4 as the fuel. Previous experiments^{5,6} suggested that the injected gas should have as low a molecular weight as possible. To test this hypothesis with pyrotechnics, fumer mixes with MgH_2 , ZrH_2 , or NaBH_4 were made up with $\text{Sr}(\text{NO}_3)_2$ as the oxidizer. Only the fumer mixes with NaBH_4 ignited and burned in the wind tunnel, although all the hydrides burned under laboratory conditions. Two of the NaBH_4 mixes yielded rapidly igniting, step-like pressure histories from which burning rates could be inferred. These two runs are summarized below and the base pressure increases vs I plotted in Figure 6 with the previous data for R20C.

<u>Fumer Mix, percent by weight</u>	<u>\dot{m}_f, g/s</u>	<u>I</u>	<u>$\Delta(P_b/P_\infty)$</u>	<u>r, cm/s</u>
15/85 $\text{NaBH}_4/\text{Sr}(\text{NO}_3)_2$	6.7	0.018	0.26	1.3
25/75 $\text{NaBH}_4/\text{Sr}(\text{NO}_3)_2$	4.8	0.013	0.23	1.0

The faster burning 15/85 $\text{NaBH}_4/\text{Sr}(\text{NO}_3)_2$ provides the largest base pressure rise observed in these wind tunnel tests. The base pressure rise for spinning R20C is 0.24 vs 0.26 for the NaBH_4 mix. It appears nonetheless, that the values for NaBH_4 fit into the trend of base pressure rise vs I exhibited by the R20C runs (Figure 6). The trend of a maximum base pressure rise for a given value of I followed by decreasing base pressure rise as I increases is also observed for gases injected into the wake (e.g., Figure 4).

⁵ J. E. Bowman and W. A. Clayden, "Reduction of Base Drag by Gas Ejection," RARDE Report 4/69, December 1969.

⁶ S. N. B. Murthy and J. R. Osborn, "Base Flow Data With and Without Injection: Bibliography and Semi-Rational Correlations," BRL Contract Report No. 113, August 1973, (AD #914188L).

REID AND HASTINGS
UPSTREAM CENTRE BODY

$M_\infty = 2$

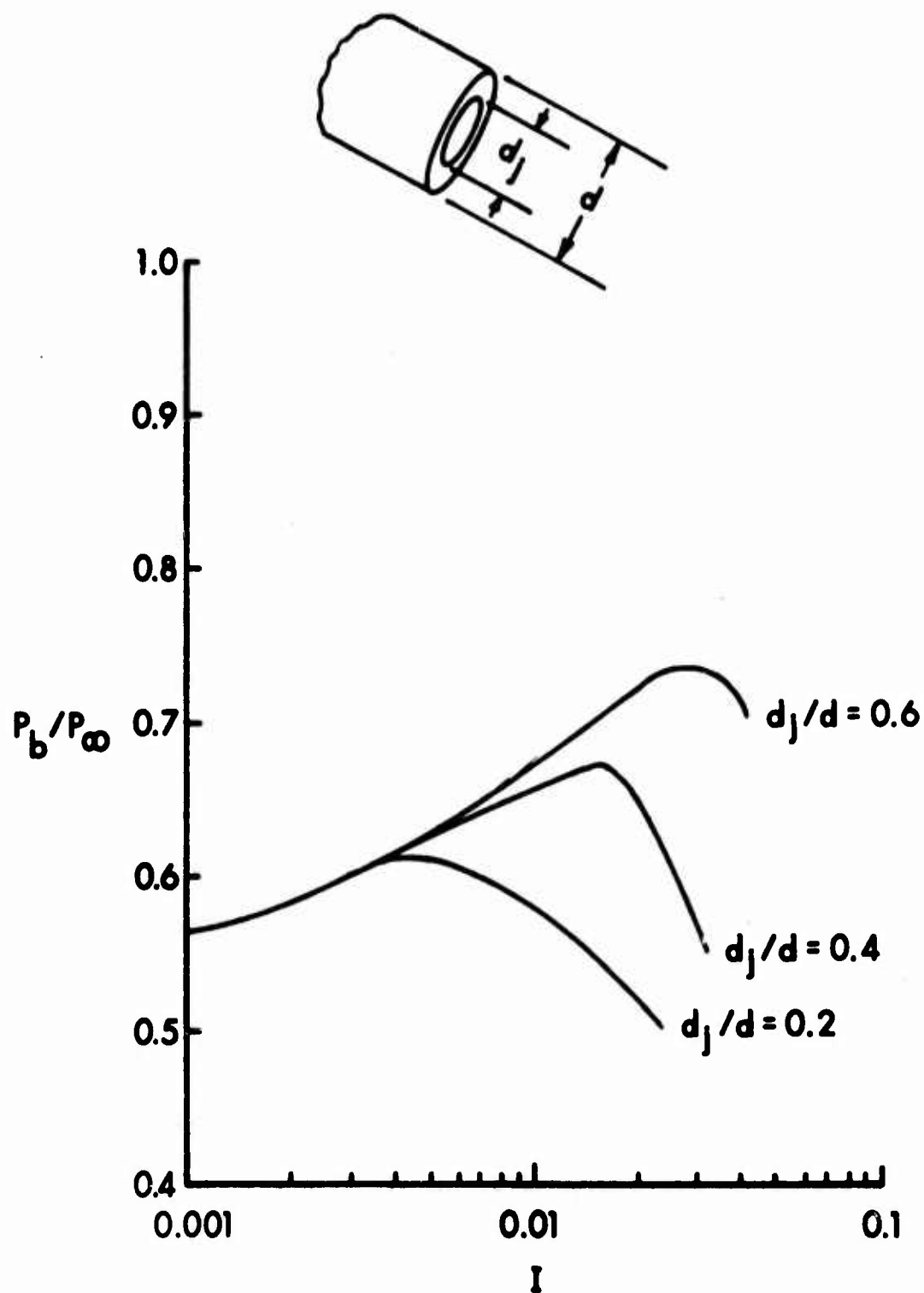


Figure 4. Summary of Reid and Hastings' Results with Various Values of d_f/d vs I

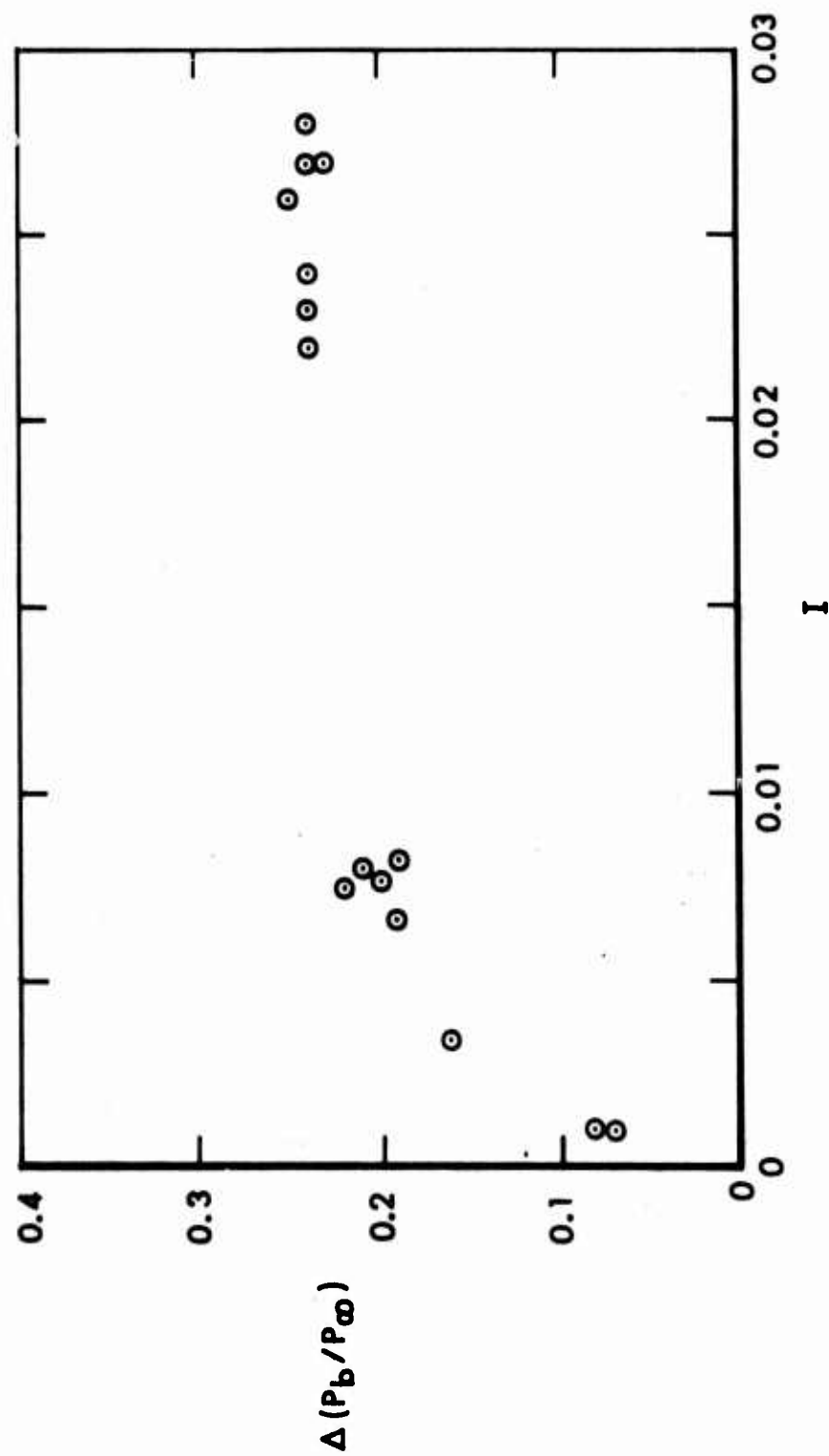


Figure 5. Increase in Base Pressure vs I for R20C

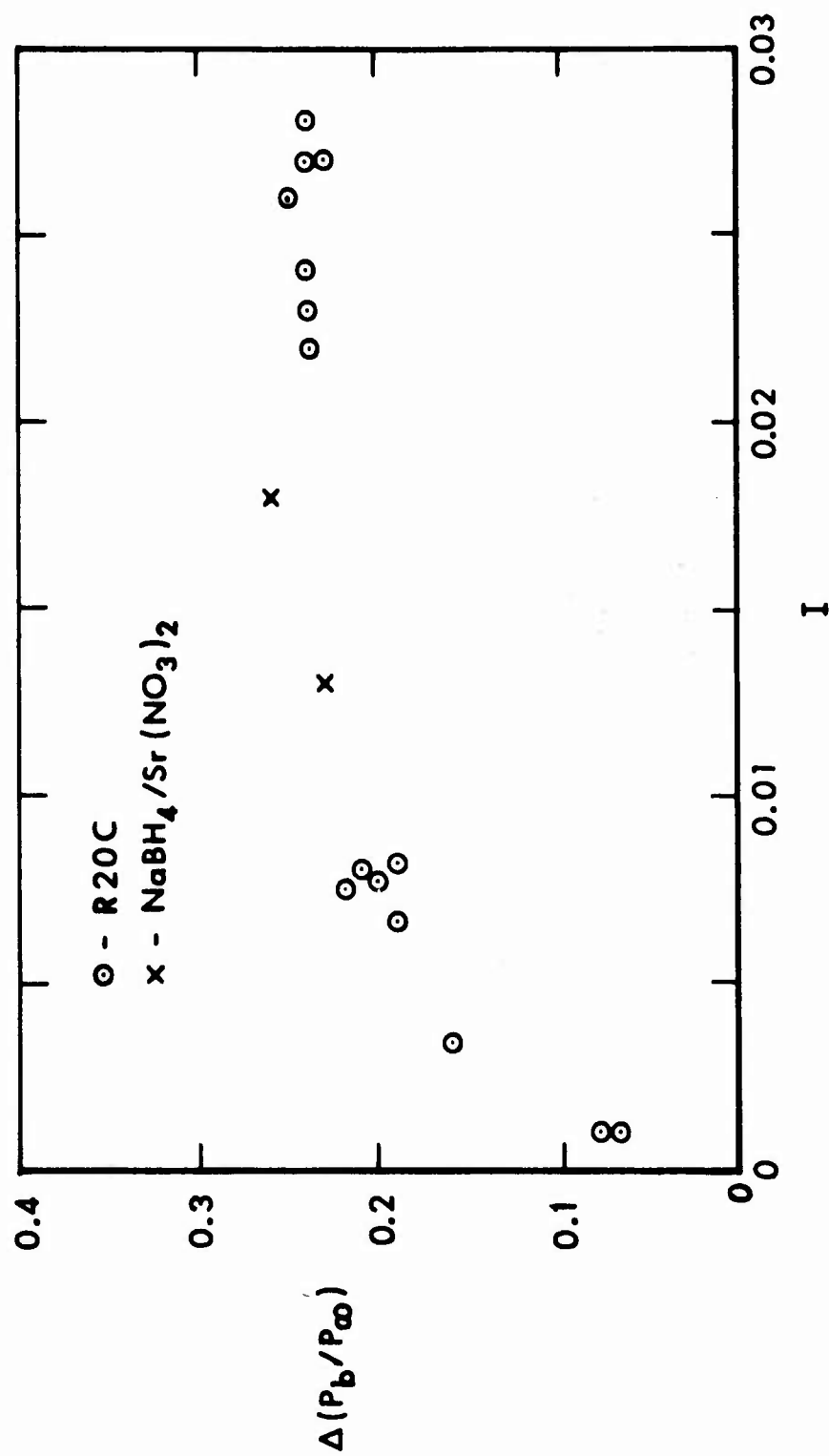


Figure 6. Increase in Base Pressure vs I for R20C and $\text{NaBH}_4/\text{Sr}(\text{NO}_3)_2$

The only other fumer mix for which quantitative computer output was available was a proprietary mix containing ammonium perchlorate (AP) and strontium nitrate as the oxidizers. The $\Delta(P_b/P_\infty)$ for this mix is plotted in Figure 7 along with the base pressure increases for the mixes in Figure 6.

The marked increase in base pressure exhibited by fumer mixes with I values near 0.001-0.002 is reflected in the specific impulses for the fumer mixes in Table IV. The specific impulses are listed in Table III; the specific impulses listed for the NaBH₄-mixes and the AP-mix include the igniter. To estimate the specific impulse for the fumer mix itself, the specific impulse values in Table III are corrected as follows:

$$I_{sp_f} = I_{sp_{(f+ig)}} \frac{t_{b_f}}{t_{b_{(f+ig)}}} \frac{m_{(f+ig)}}{m_f} \quad (4)$$

A summary of the specific impulses for the fumer mixes in Table IV is presented in Table V and the specific impulses as a function of I are plotted in Figure 8. The maximum specific impulse occurs at relatively low values of I (approximately 0.002). In a situation where the quantity of fumer that can be added to a projectile is limited, the appropriate fumer mix should be one with an injection parameter near 0.002.

The next step in the analysis of the correlation between base pressure increase and the injection parameter is to see if a function can be found relating the base drag reduction to I. Bowman and Clayden⁵ proposed the following expression for that purpose

$$C_{Db} = C_{Db_i} e^{-JxI} \quad (5)$$

The constant J varies with Mach number, and the temperature and molecular weight of the injected gas.

Bowman and Clayden stated that they were interested in a simple, empirical expression for use in systems analysis and their expression should be regarded as "tentative." From the results for pyrotechnic combustion, Bowman and Clayden's simple expression appears inadequate. Equation (5) implies that the base drag disappears at large values of I; this is not true for the pyrotechnics nor for ejection of various gases (e.g., Figure 4). Equation (5) should be more properly expressed as

$$C_{Db} = C_{Db_{min}} + (C_{Db_i} - C_{Db_{min}}) e^{-JxI}, \quad (6)$$

where $C_{Db_{min}}$ is the minimum base drag coefficient that may be achieved.

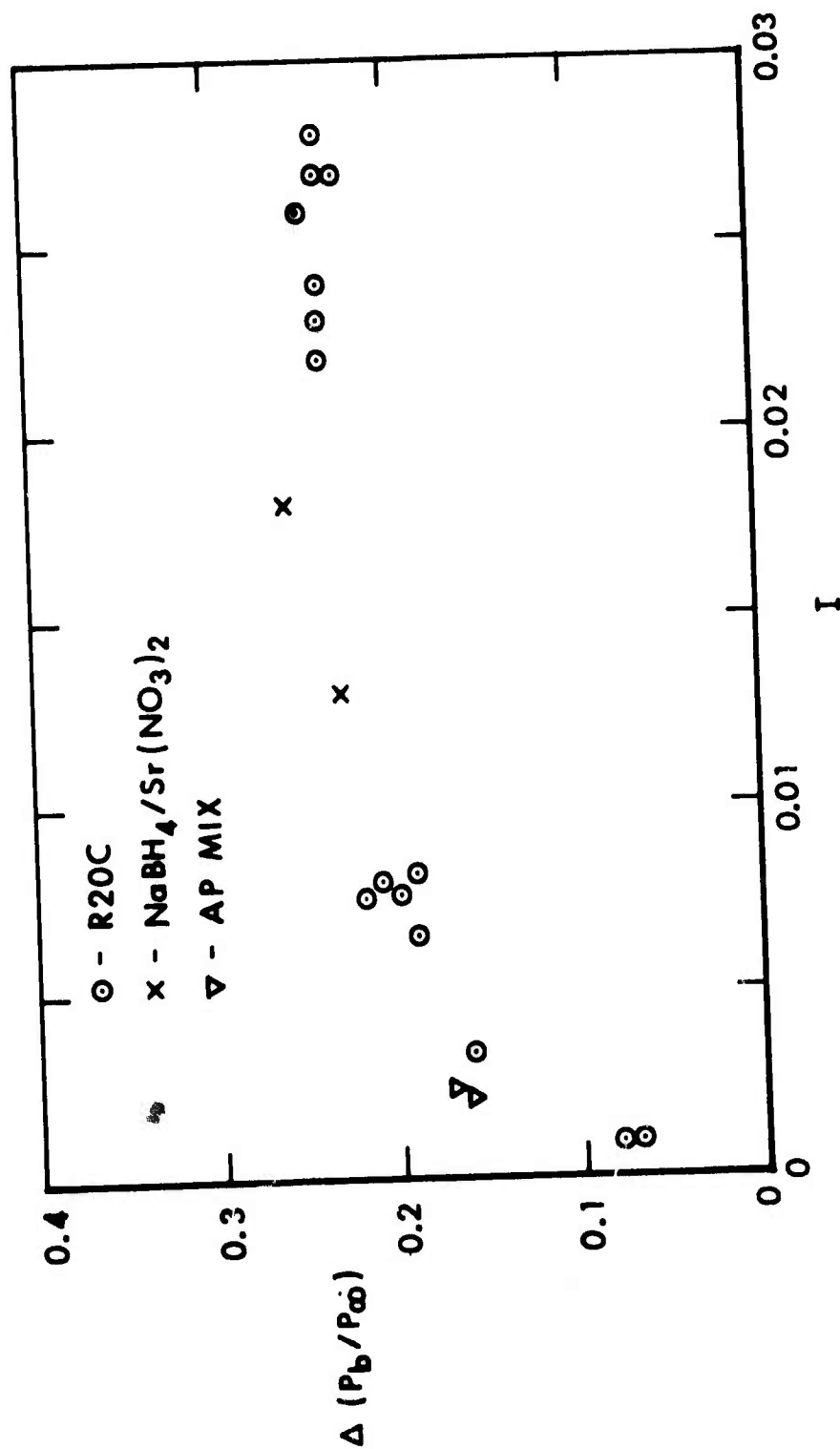


Figure 7. Increase in Base Pressure vs I for R20C, $\text{NaBH}_4/\text{Sr}(\text{NO}_3)_2$, and AP-Mix

TABLE V. Specific Impulses of Fumer Mixes in Table IV

<u>Fumer Mix</u>	<u>Isp, kN-s/kg</u>	<u>I x 10³</u>	<u>Reference</u>
R20C	6.8	1.0	a
R20C	7.1	1.0	a
R20C	4.4	3.4	b
R20C	3.0	6.7	b
R20C	3.4	7.5	b
R20C	3.2	8.0	c
R20C	2.2	8.2	b
R20C	2.6	8.7	b
R20C	1.2	23.0	b
R20C	1.4	23.0	b
R20C	0.95	24.0	b
R20C	0.94	26.0	b
R20C	1.1	27.0	b
R20C	1.3	27.0	b
R20C	1.1	28.0	b
AP-mix	7.8 ^d	2.2	a
AP-mix	7.2 ^d	2.4	a
NaBH ₄ /Sr(NO ₃) ₂ (15/85)	1.2 ^d	18.0	a
NaBH ₄ /Sr(NO ₃) ₂ (25/75)	1.8 ^d	13.0	a

^a This work. ^b F. P. Baltakis, "Wind Tunnel Study of Projectile Base Drag Reduction Through Combustion of Solid, Fuel-Rich Propellants," NOL Wind Tunnel Report No. 93, October 1974. ^c Reference 1.

^d Corrected value using Eq. (4).

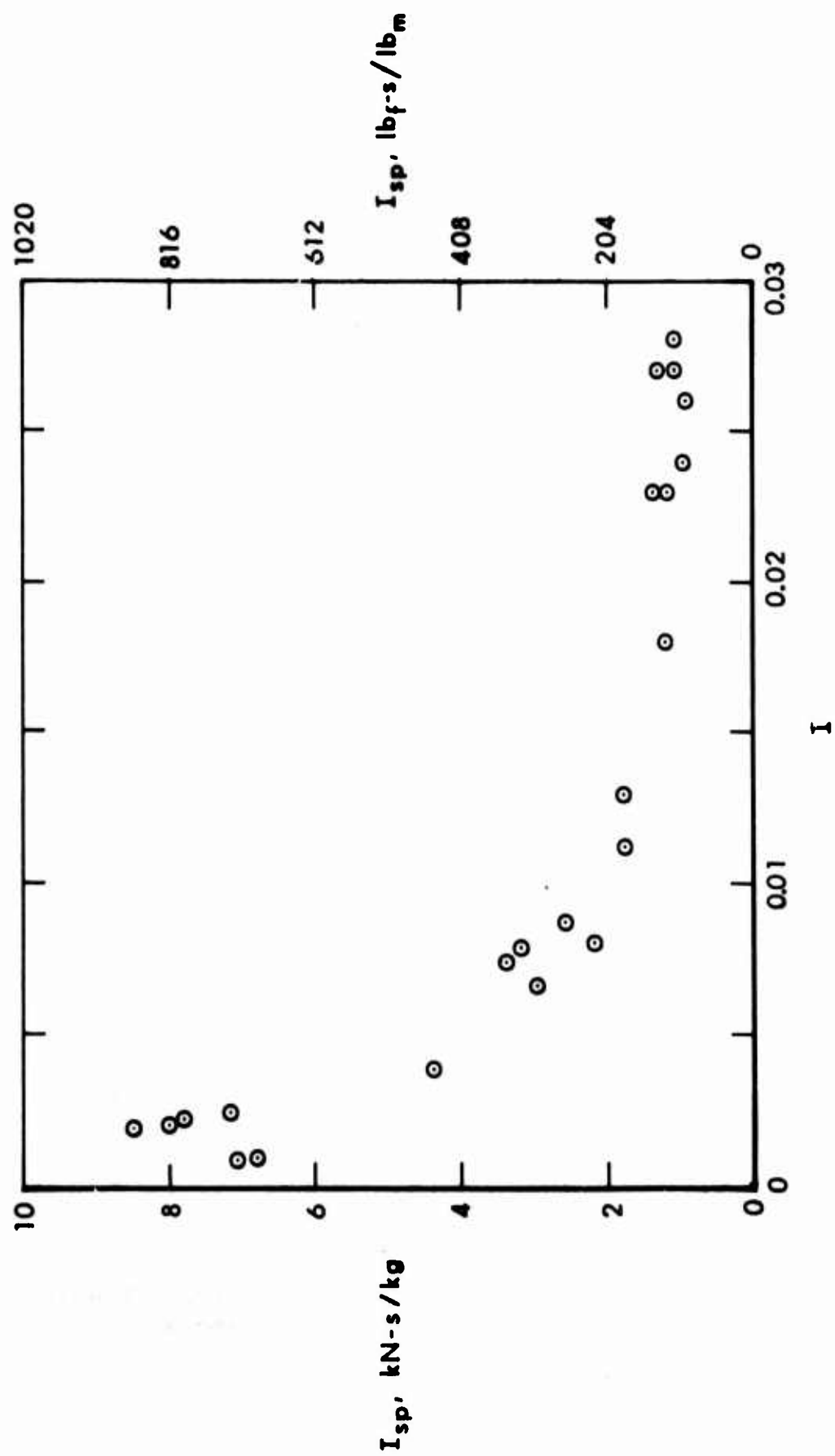


Figure 8. Specific Impulse vs I for Fumer Mixes from Table IV, $M_\infty = 2.0$

To test the applicability of equations (5) and (6) to the data generated in the wind tunnel tests, equations (5) and (6) were expressed in terms of $\Delta(P_b/P_\infty)$ through

$$C_{Db} = \frac{2(P_\infty - P_b)}{\rho_\infty U_\infty^2} \quad (7)$$

Equations (5) and (6) become

$$\Delta\left(\frac{P_b}{P_\infty}\right) = \left[1 - \left(\frac{P_b}{P_\infty}\right)_i\right] [1 - e^{-JxI}] \quad , \text{ and} \quad (8)$$

$$\Delta\left(\frac{P_b}{P_\infty}\right) = \Delta\left(\frac{P_b}{P_\infty}\right)_{\max} (1 - e^{-JxI}) \quad , \quad (9)$$

where $\Delta\left(\frac{P_b}{P_\infty}\right)_{\max}$ refers to the maximum base pressure that may be achieved.

A non-linear least-squares program⁷ was used to fit equations (8) and (9) to the data in Figure 7. In equation (8), the initial value of P_b/P_∞ was 0.62. The best-fit value of J was computed for equation (8); for equation (9) best-fit values of J and $\Delta(P_b/P_\infty)_{\max}$ were computed. The results of the calculations are presented below and the curves generated using the best-fit values are drawn through the experimental data in Figure 9.

Equation	J	$\Delta(P_b/P_\infty)_{\max}$
(8)	66	-
(9)	3.9×10^2	0.23

Equation (8) underestimates the $\Delta(P_b/P_\infty)$ at low values of I and overestimates the base pressure increase at larger values of I . Equation (9) fits the experimental data much better, although the best-fit $\Delta(P_b/P_\infty)_{\max}$ is less than the 0.26 recorded for the (15/85) $\text{NaBH}_4/\text{Sr}(\text{NO}_3)_2$ mix.

An alternate expression that also fits the experimental data as well as equation (9) is the following

$$\Delta(P_b/P_\infty) = \frac{QI}{1+NI} \quad , \quad (10)$$

⁷ R. H. Moore and R. K. Ziegler, "The Solution of the General Least Squares Problem With Special Reference to High-Speed Computers," Los Alamos Scientific Laboratory Report LA-2367, March 1960.

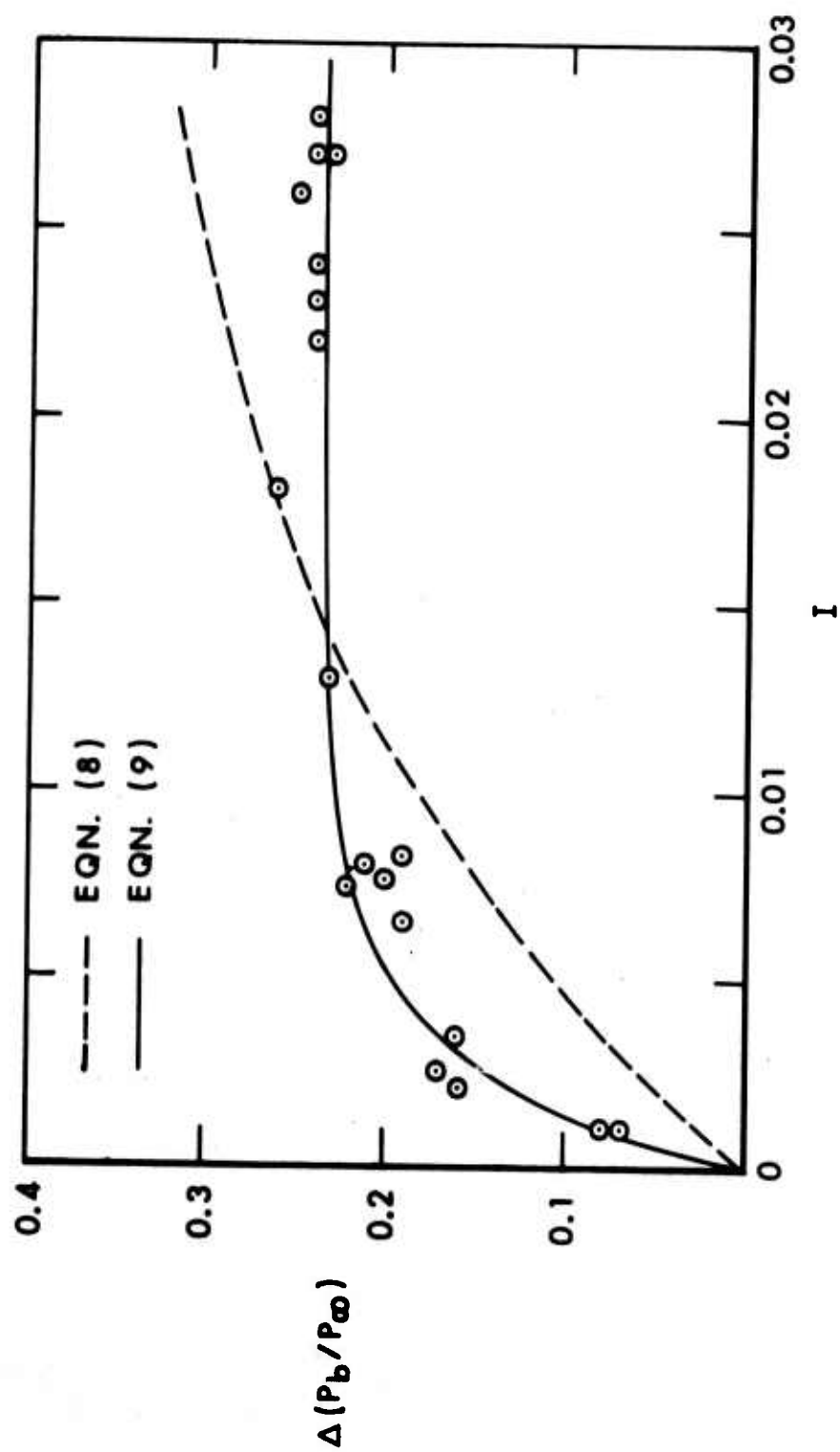


Figure 9. Increase in Base Pressure vs I

where Q and N are the floating parameters. In Figure 10 the curve generated from best-fit values of Q and N is drawn through the experimental points. For the data taken from Figure 7, best-fit values of Q and N are 1.4×10^2 and 5.2×10^2 , respectively.

The remaining test runs in Table IV that merit discussion are those test runs made with the force balance. The object of these runs was to compare the specific impulses computed from the base pressure measurements with the specific impulses determined experimentally. Table VI compares specific impulses measured with R20C as the fumer mix with specific impulses computed from the base pressure measurements. The measured and computed specific impulses are in reasonable agreement. Thus, it appears the pressure distribution over the rear face of the wind tunnel model is uniform. Kayser⁴ measured the pressure distribution over the face of his model while gas was being injected into the wake region and he found that the pressure increase was uniform.

The remaining tests can be treated only qualitatively either because the combustion of the fumer was irregular or because quantitative computer output was not available. In order to summarize these tests in a systematic manner, Table VII was constructed. For each combination of fuel and oxidizer, the following information is provided:

- a. Run number.
- b. Percent by weight of fuel.
- c. Comment on the burning properties:
 - N - no combustion.
 - B - unsteady burning.
 - Q - smooth combustion, no quantitative output.
 - IV - smooth combustion, quantitative output, listed in Table IV.

For the tests in Table VII listed as smooth burning but with no quantitative output, the percent base drag reduction and injection parameter are listed in Table VIII. The longer the fumer mix burned, the less important is the failure to account for the igniter. For example, the injection parameter for Run 66 (AP-mix) changes only slightly when the correction is made for the igniter as shown below:

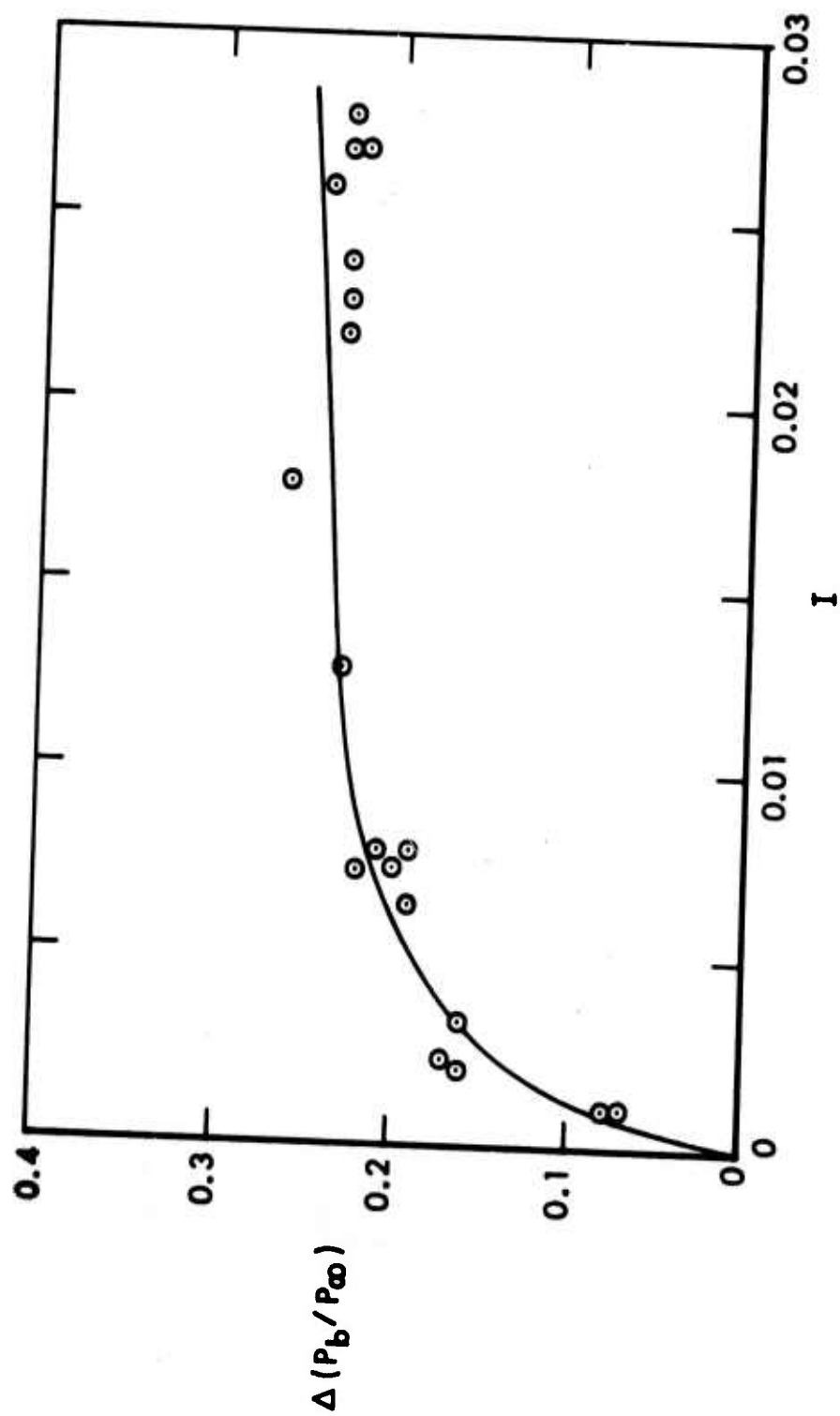


Figure 10. Increase in Base Pressure vs I with Equation (10)

TABLE VI. Comparison Between Specific Impulses Measured
by the Force Balance with those Inferred from Pressure Orifices^a

<u>Run</u>	<u>\dot{m}, g/s</u>	<u>I</u>	<u>Isp, kN-s/kg</u>	<u>Reference</u>
51(F) ^b	3.1	8.8	3.2	d
52(F)	3.3	9.7	3.1	d
53(F)	3.3	8.8	2.5	d
1(P) ^c	4.0	8.0	3.2	e
117(P)	3.6	8.0	3.2	f
119(P)	3.1	6.7	3.0	f
121(P)	3.7	8.2	2.2	f
112(P)	3.4	7.5	3.4	f
124(P)	4.0	8.7	2.6	f

^a Fumer mix is R20C, $M_{\infty} = 1.98$ or 1.99

^b Specific impulse determined from force balance measurements.

^c Specific impulse determined from pressure measurements.

^d This work.

^e Reference 1.

^f F. P. Baltakis, "Wind Tunnel Study of Projectile Base Drag Reduction Through Combustion of Solid, Fuel-Rich Propellants," NOL Wind Tunnel Report No. 93, October 1974.

TABLE VII. Summary of Results for Various
Fuel/Oxidizer Combinations Tested^a

<u>Oxidizer</u>	<u>BaCrO₄</u>	<u>KClO₄</u>	<u>KClO₄/C.R.^b</u>	<u>Sr(NO₃)₂</u>	<u>Sr(NO₃)₂/C.R.</u>
Fuel					
B	70/15/N	71/31/B 94/31/B			
NaBH ₄				56/15/IV 57/25/IV 68/25/Q 58/35/B 69/35/B 54/40/B 83/40/Q	
Mg			77/37/Q 79/37/Q		
Ti		76/33/N 90/33/N	86/30/B	80/36/N 89/36/B	81/32/Q
Zr		74/57/Q	75/51/N	78/52/B	73/47/Q
MgH ₂				61/24/N	
ZrH ₂				59/70/N 60/50/N 84/50/N	

^aThe three terms represent: run number/percent by weight of fuel/
burning characteristic of the mix, IV - smooth burning, quantitative
computer output available, Q-smooth burning, no quantitative computer
output available; B-uneven combustion or poor ignition, N-failed to
ignite.

^bTernary mix containing 10% by weight calcium resinate.

Table VIII. Injection Parameters and Base Drag Reductions
for Smooth-Burning Mixes with No Quantitative Computer Output

<u>Run</u>	<u>Composition</u>	<u>I</u>	<u>%ΔC_{Db} reduced</u>
68	$\text{NaBH}_4/\text{Sr}(\text{NO}_3)_2$ (25/75)	0.011	45
83	$\text{NaBH}_4/\text{Sr}(\text{NO}_3)_2$ (40/75)	0.005	51
77	$\text{Mg}/\text{KClO}_4/\text{C.R.}^b$ (37/53/10)	0.002	31
79	$\text{Mg}/\text{KClO}_4/\text{C.R.}$ (37/53/10)	0.003	46
81	$\text{Ti}/\text{Sr}(\text{NO}_3)_2/\text{C.R.}$ (32/58/10)	0.012	57
74	Zr/KClO_4 (57/43)	0.019	59
73	$\text{Zr}/\text{Sr}(\text{NO}_3)_2/\text{C.R.}$ (47/43/10)	0.003	32

<u>Run 66</u>	<u>tb, sec</u>	<u>m, g</u>	<u>I</u>
igniter + fumer	11.2	8.6	0.002
fumer	9.4	7.8	0.0022

For the faster burning mixes, the correction is more substantial as shown for a $\text{NaBH}_4/\text{Sr}(\text{NO}_3)_2$ mix.

<u>Run 56</u>	<u>tb, sec</u>	<u>m, g</u>	<u>I</u>
igniter + fumer	2.4	10.2	0.011
fumer	1.4	9.4	0.018

On this basis the results in Table VIII generally follow the trend that the faster-burning mixes yield higher base-drag reductions than the slower burning mixes.

V. CONCLUSIONS

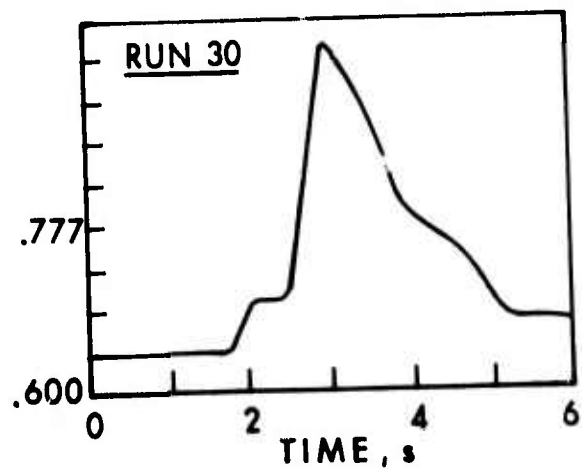
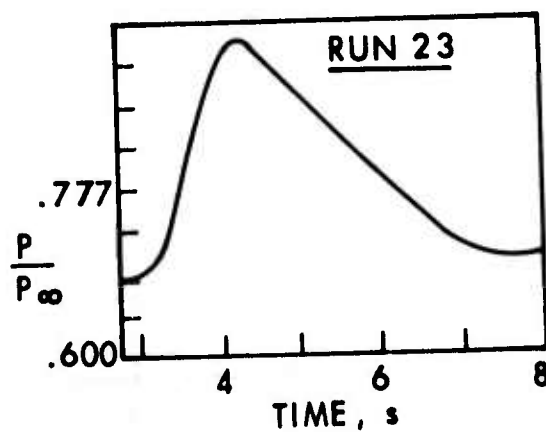
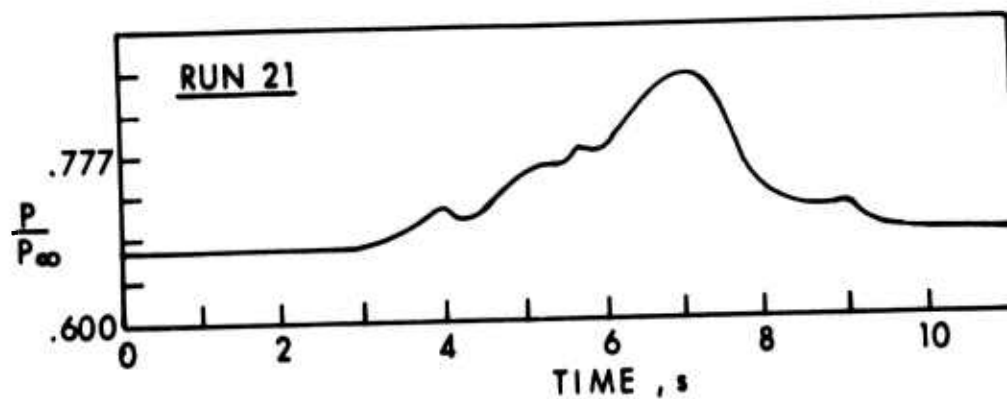
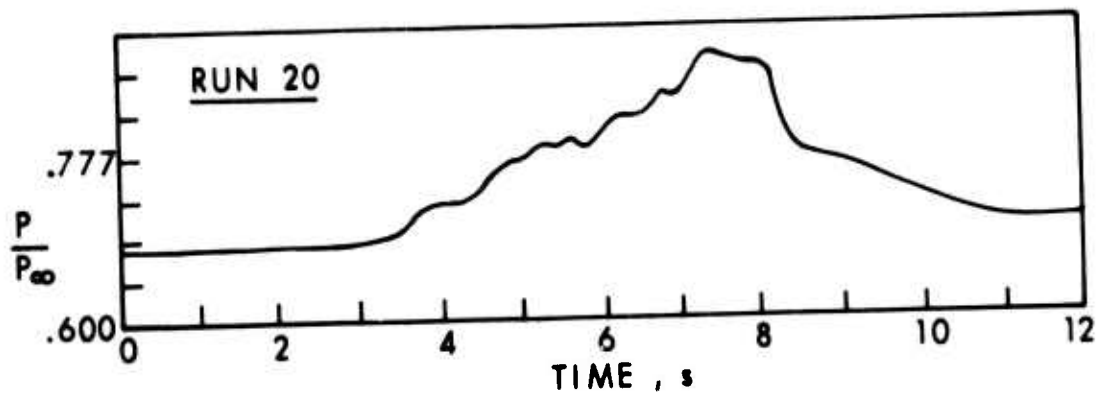
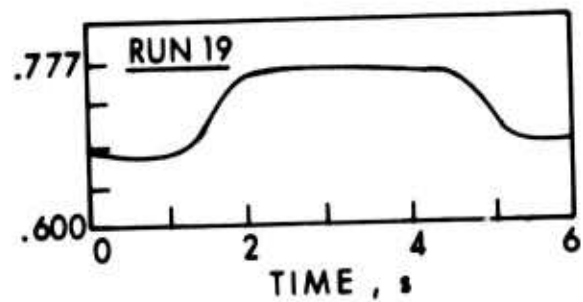
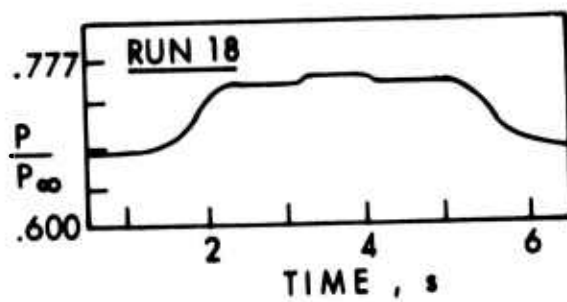
1. Base pressure increase from pyrotechnic combustion can be correlated by the injection parameter.
2. Maximum base pressure increase at $M_\infty = 2.0$ occurs near an I value of 0.002. The maximum base pressure increase corresponds to a 68% reduction in the base-drag coefficient.
3. Specific impulses of nearly 8 kN-s/kg have been observed with fumer mixes with injection parameters near 0.002.
4. Specific impulses measured with a force balance are in reasonable agreement with the specific impulse computed by integration of base pressure vs time curves. This implies the pressure distribution is uniform over the base of the wind tunnel model.
5. The use of NaBH_4 as a fuel yielded a fumer mix that burned rapidly and smoothly, but did not provide a fumer fuel much different than a magnesium-based fumer mix with the same burning rate.

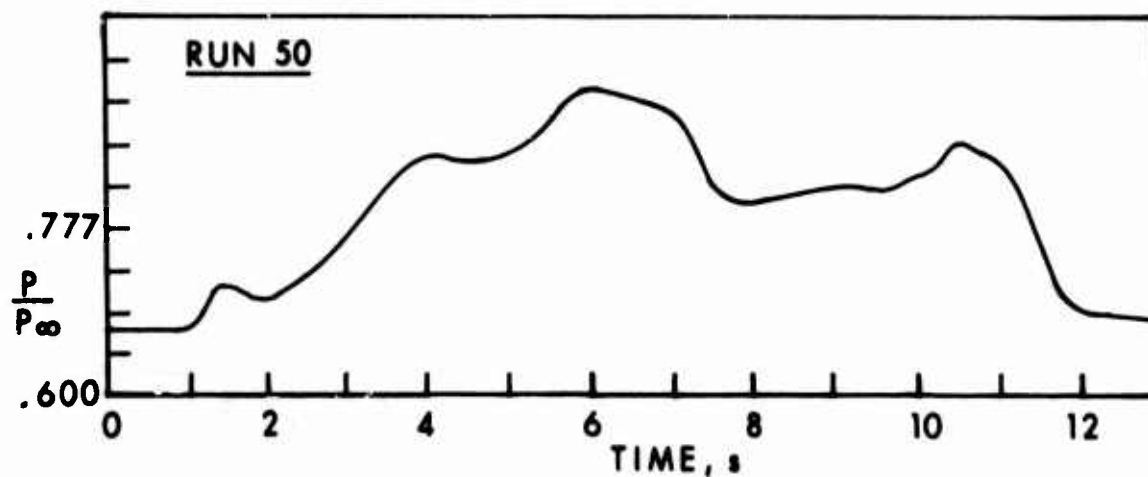
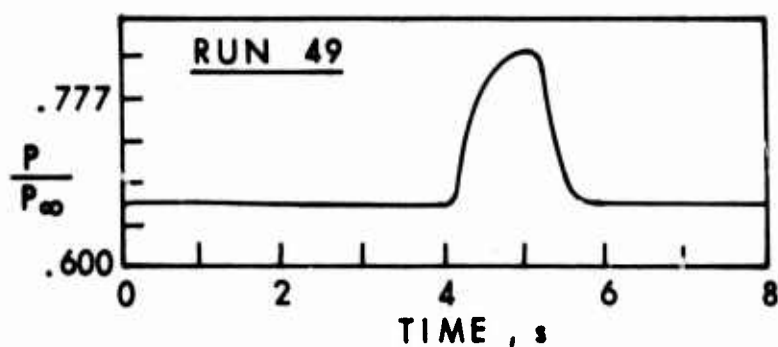
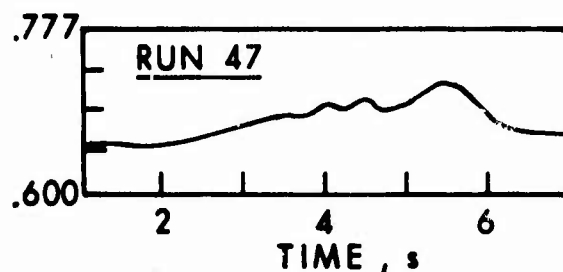
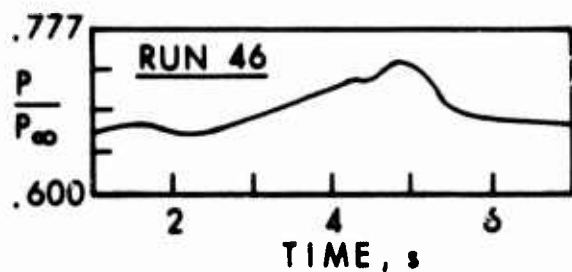
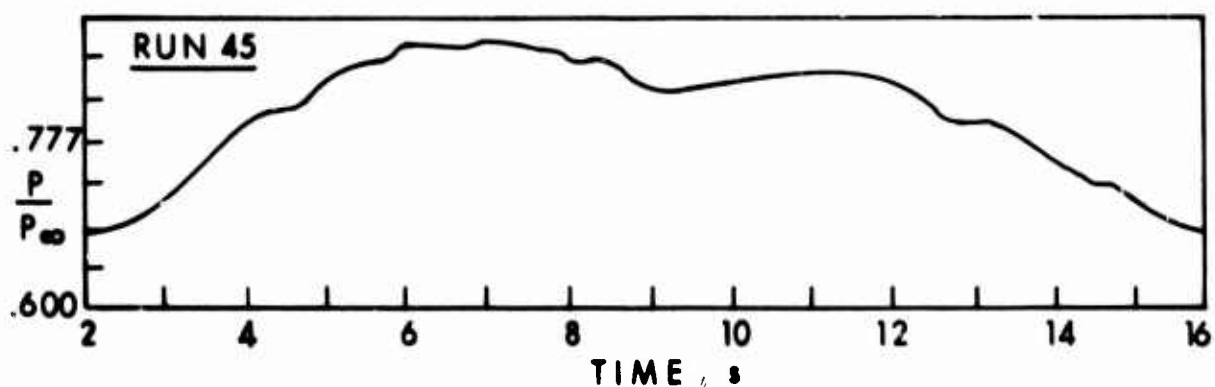
REFERENCES

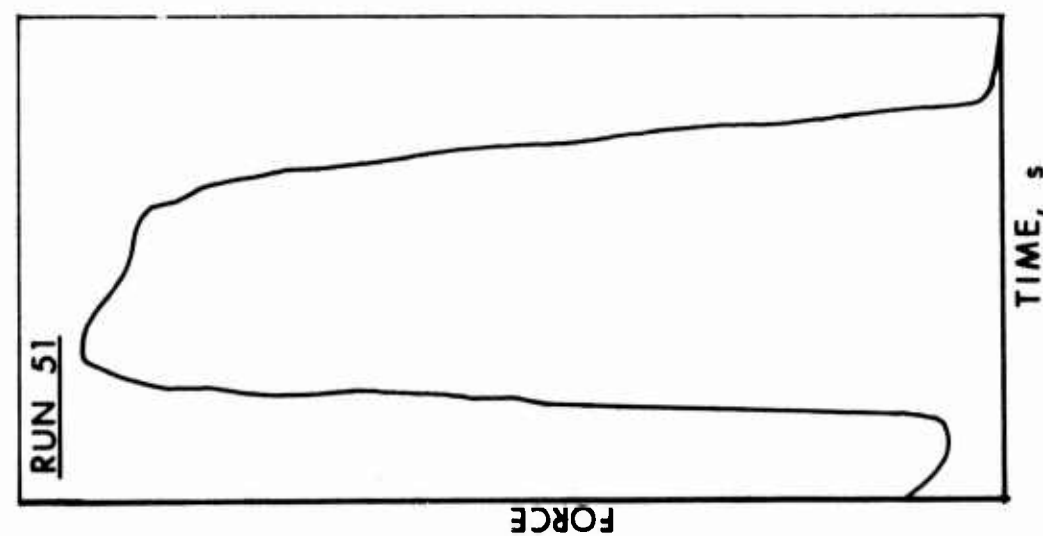
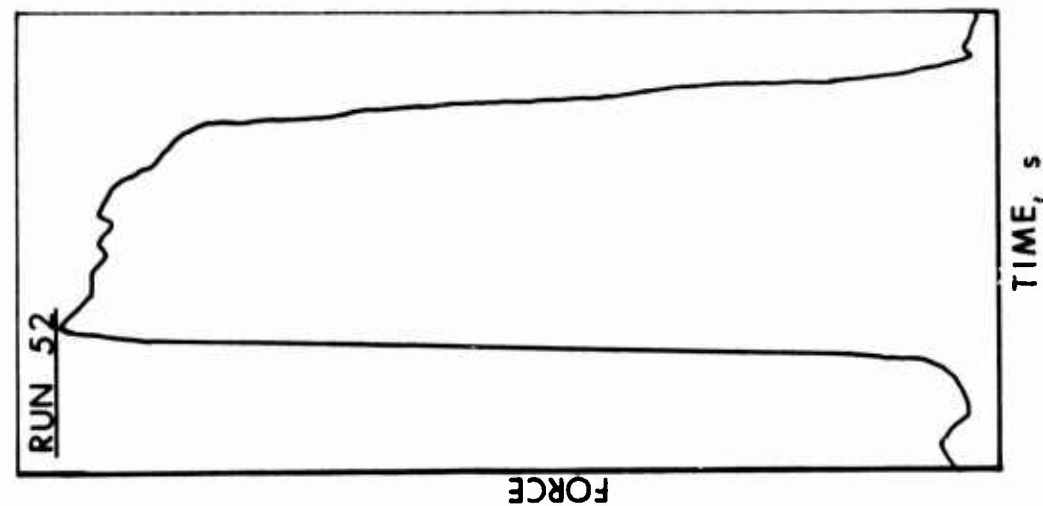
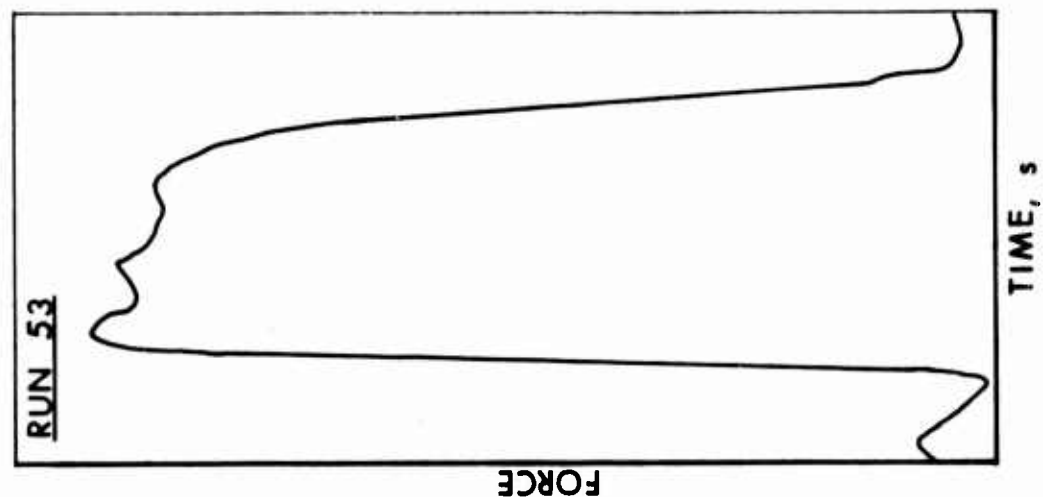
1. J. R. Ward, F. P. Baltakis, S. W. Pronchick, "Wind Tunnel Study of Base Drag Reduction by Combustion of Pyrotechnics," BRL Report No. 1745, October 1974, (AD #B000431L).
2. J. R. Ward, F. P. Baltakis, D. Mancinelli, and T. Elmendorf, "Wind Tunnel Experiments on the Effect of Combustion in the Wake Region of Supersonic Projectiles," BRL Memorandum Report 2588, February 1976, (AD #B009982L).
3. J. Reid and R. C. Hastings, "The Effect of a Central Jet on the Base Pressure of a Cylindrical Afterbody in a Supersonic Stream," RAE Report No. Aero, 2621, 1959.
4. L. D. Kayser, "Effects of Base Bleed and Supersonic Nozzle Injection on Base Pressure," BRL Memorandum Report No. 2456, March 1975, (AD #B003442L).
5. J. E. Bowman and W. A. Clayden, "Reduction of Base Drag by Gas Ejection," RARDE Report 4/69, December 1969.
6. S. N. B. Murthy and J. R. Osborn, "Base Flow Data With and Without Injection: Bibliography and Semi-Rational Correlations," BRL Contract Report No. 113, August 1973, (AD #914188L).
7. R. H. Moore and R. K. Ziegler, "The Solution of the General Least Squares Problem With Special Reference to High-Speed Computers," Los Alamos Scientific Laboratory Report LA-2367, March 1960.

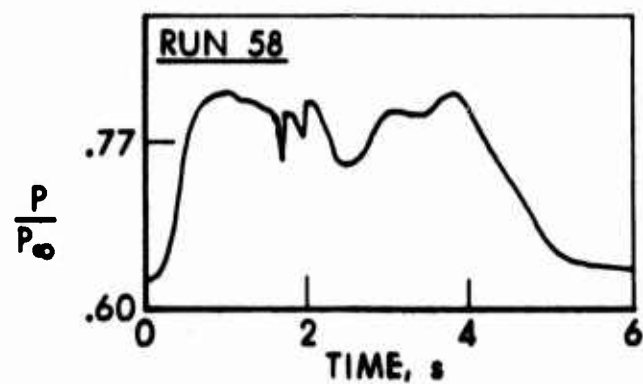
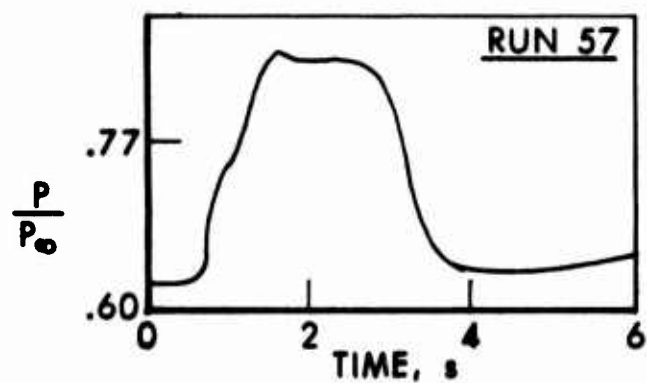
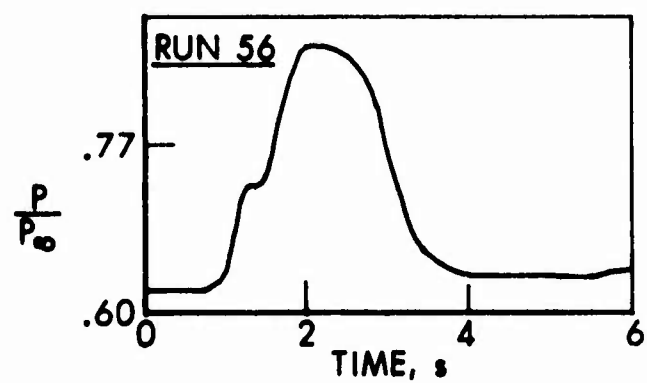
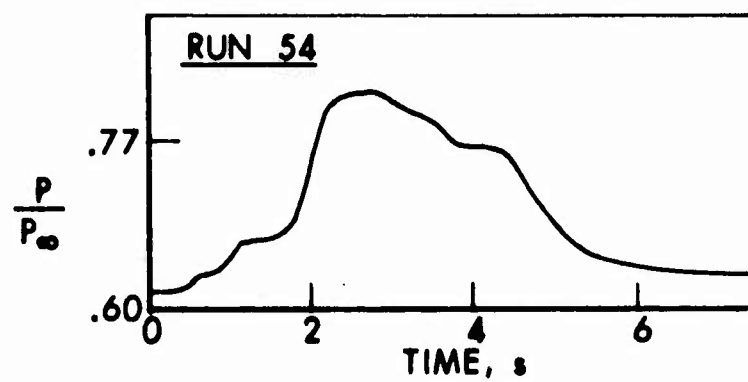
APPENDIX A

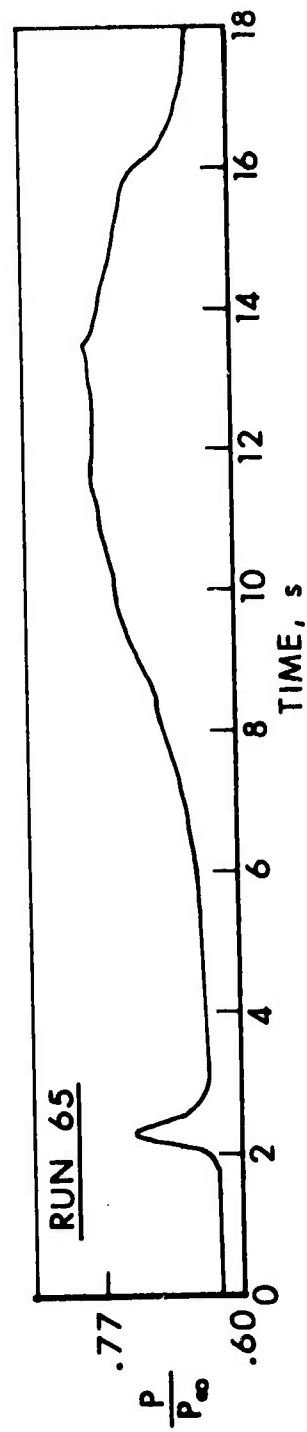
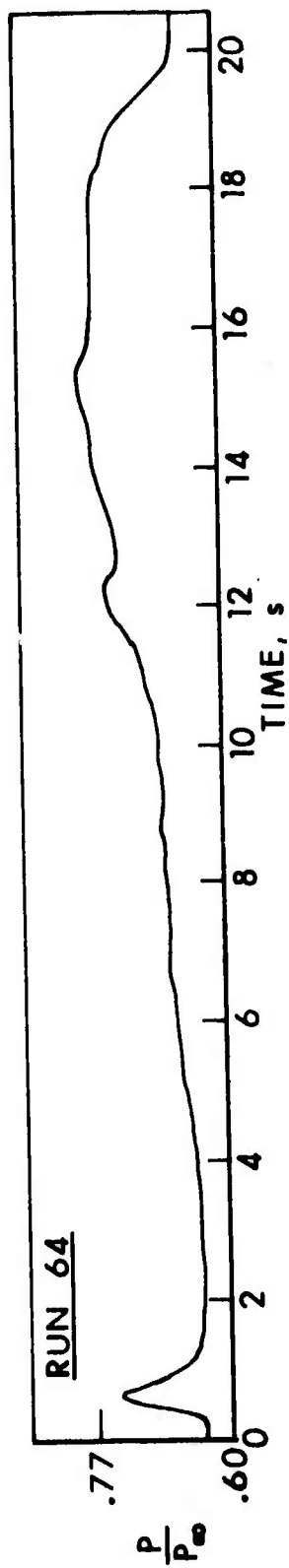
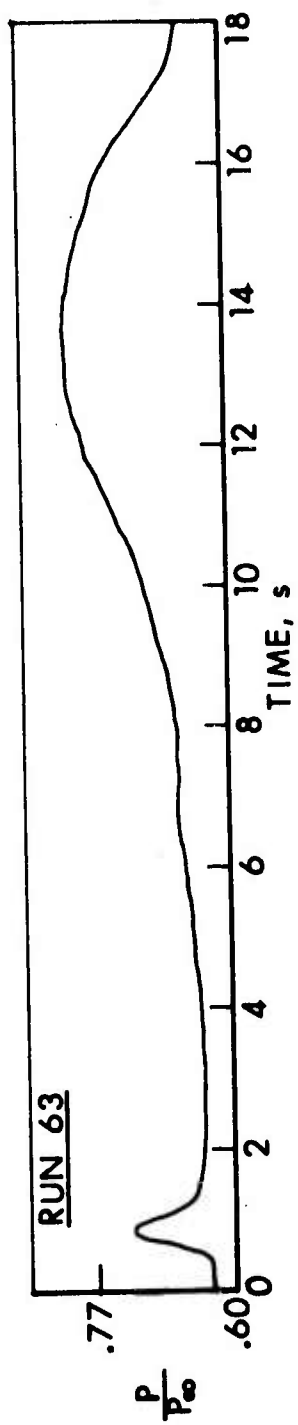
Summary of the Pressure-Time Histories for the Runs Which Ignited

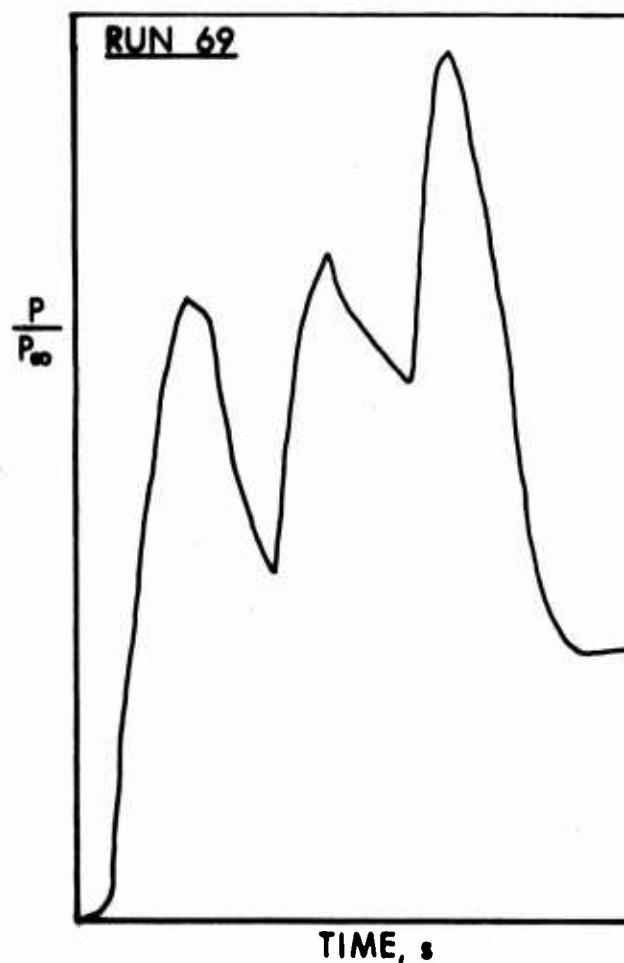
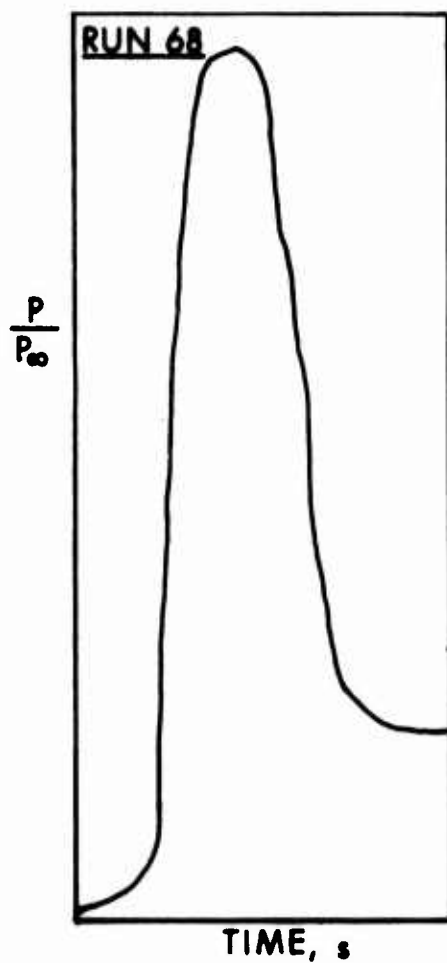
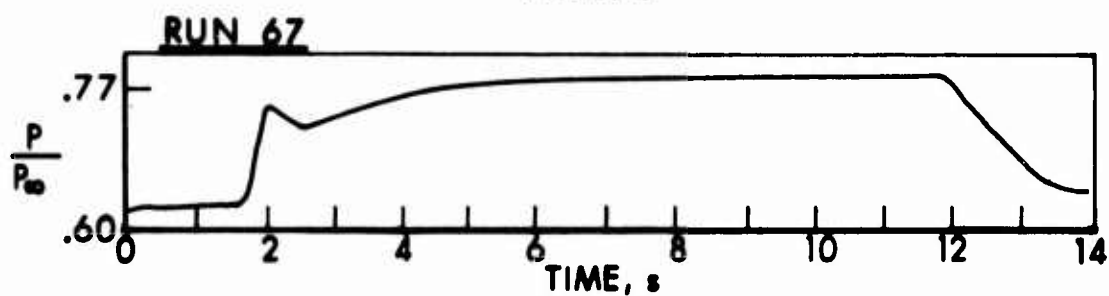
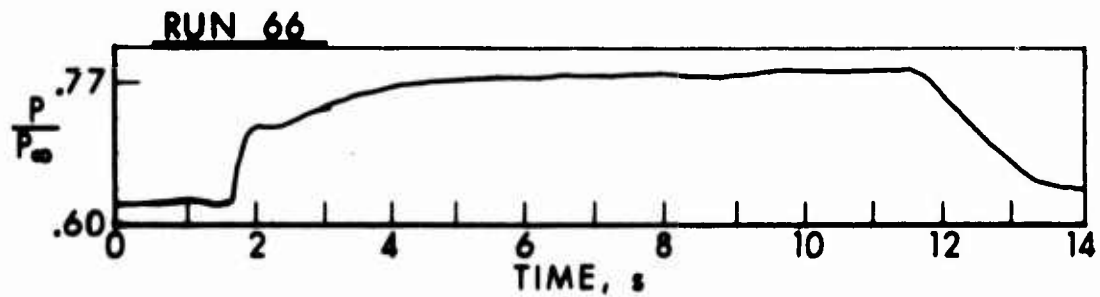


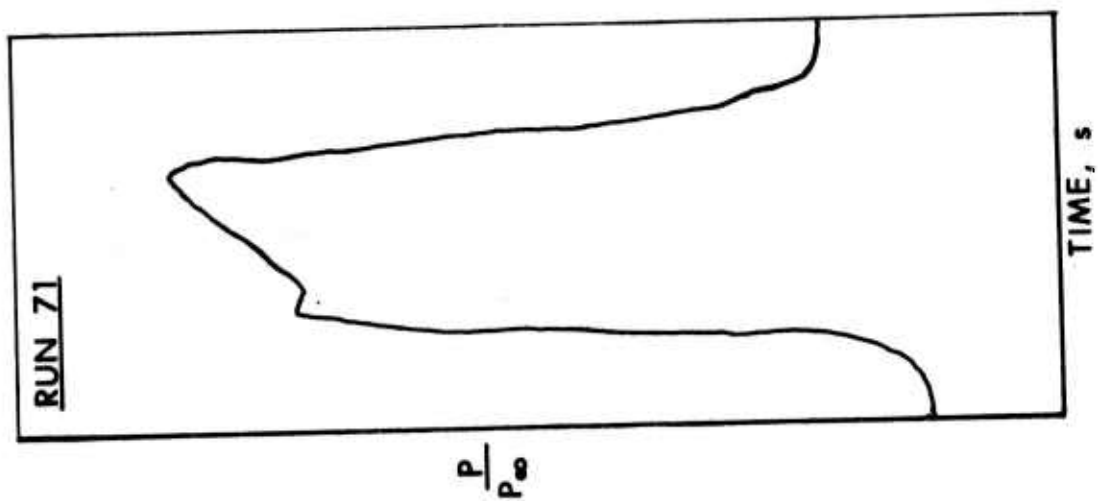
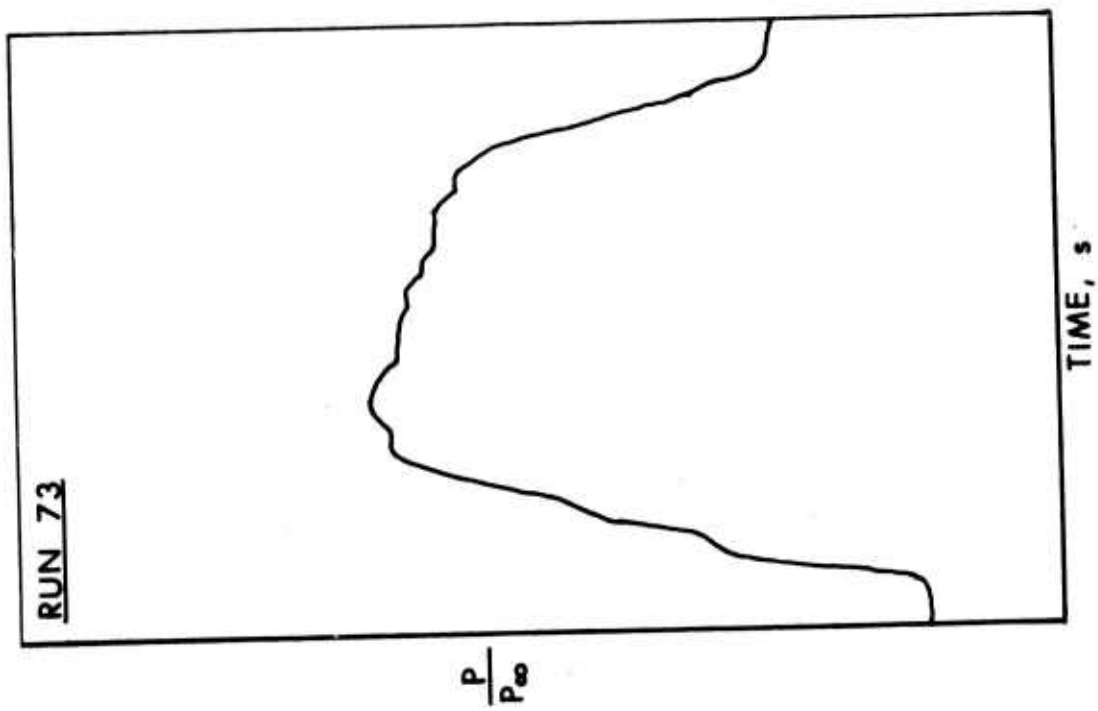
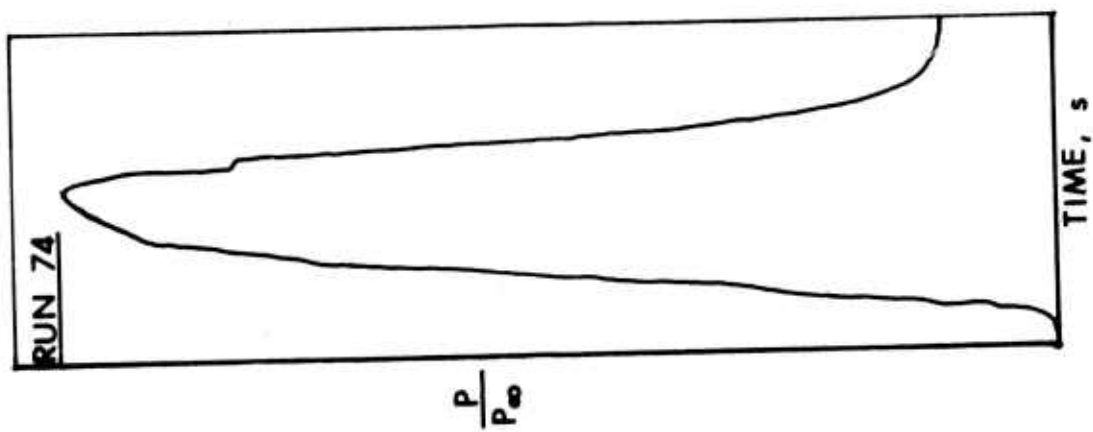


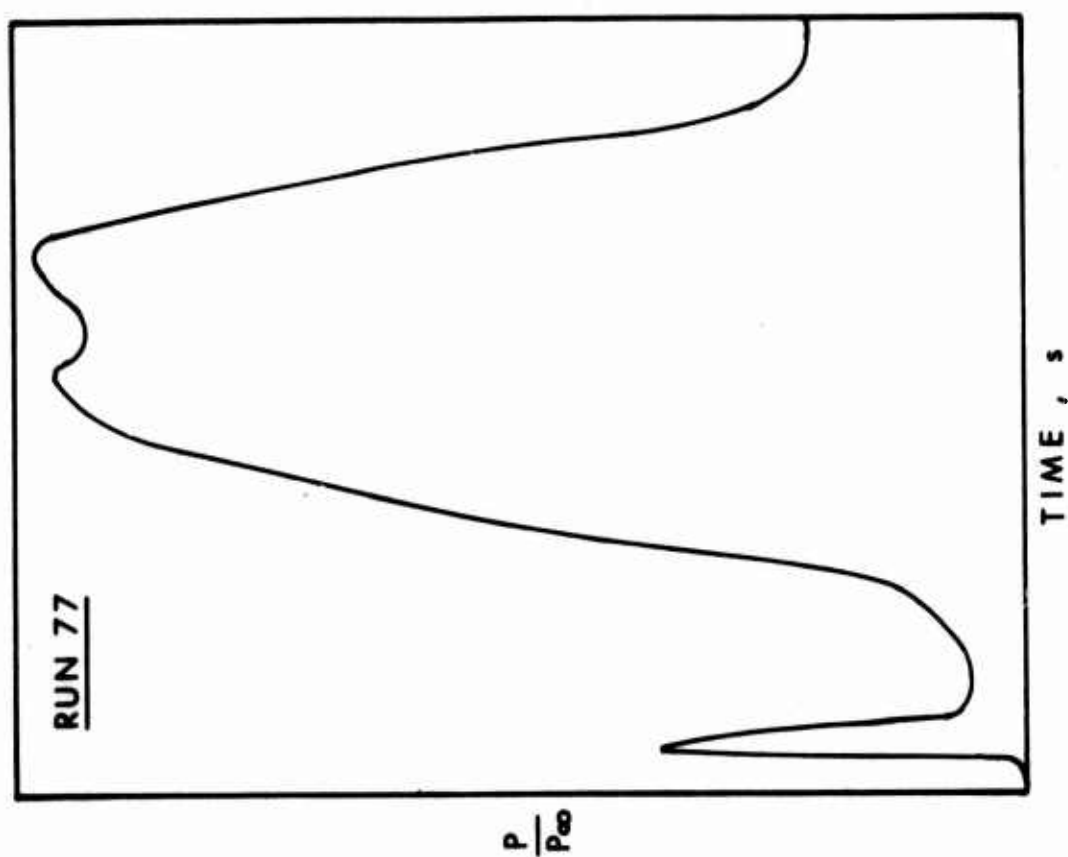
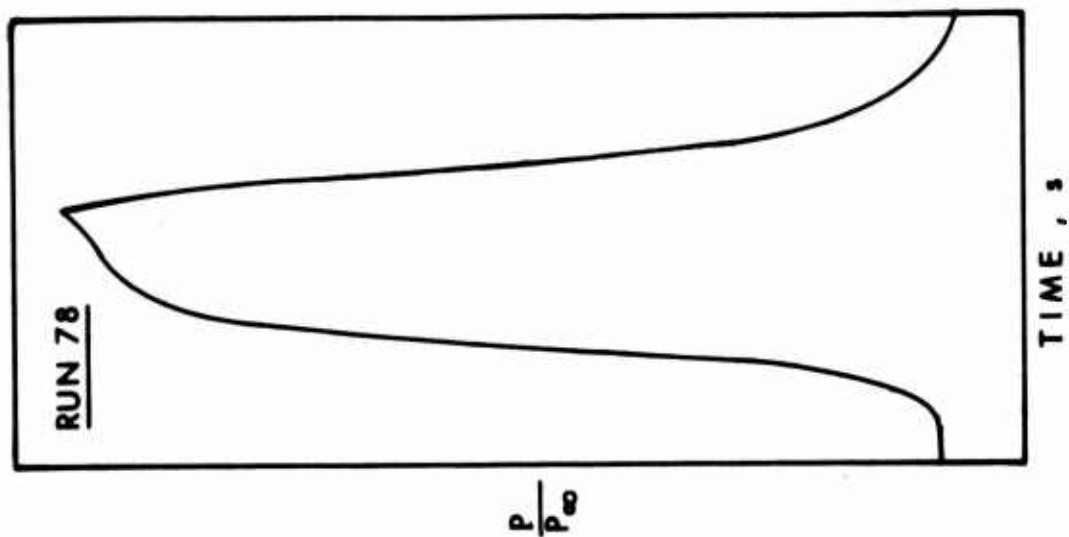


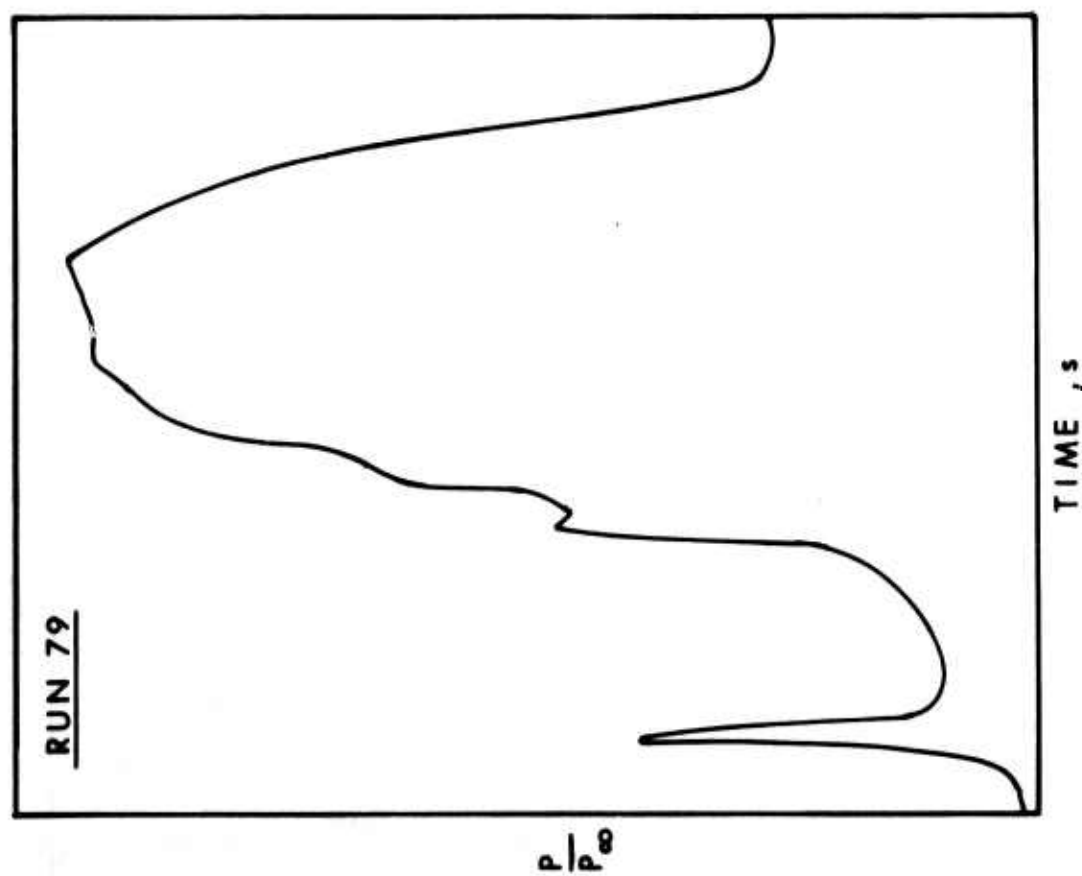
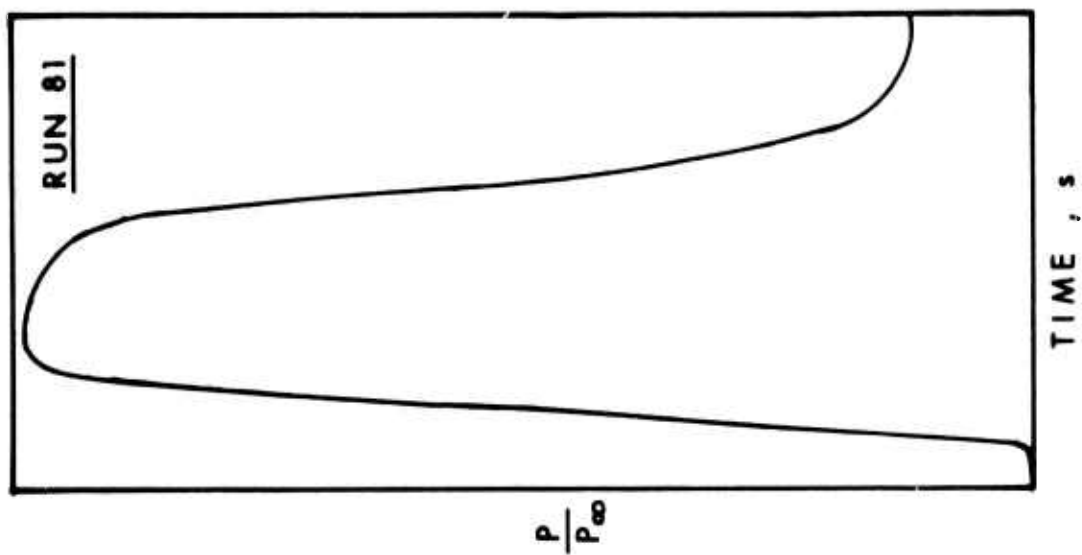


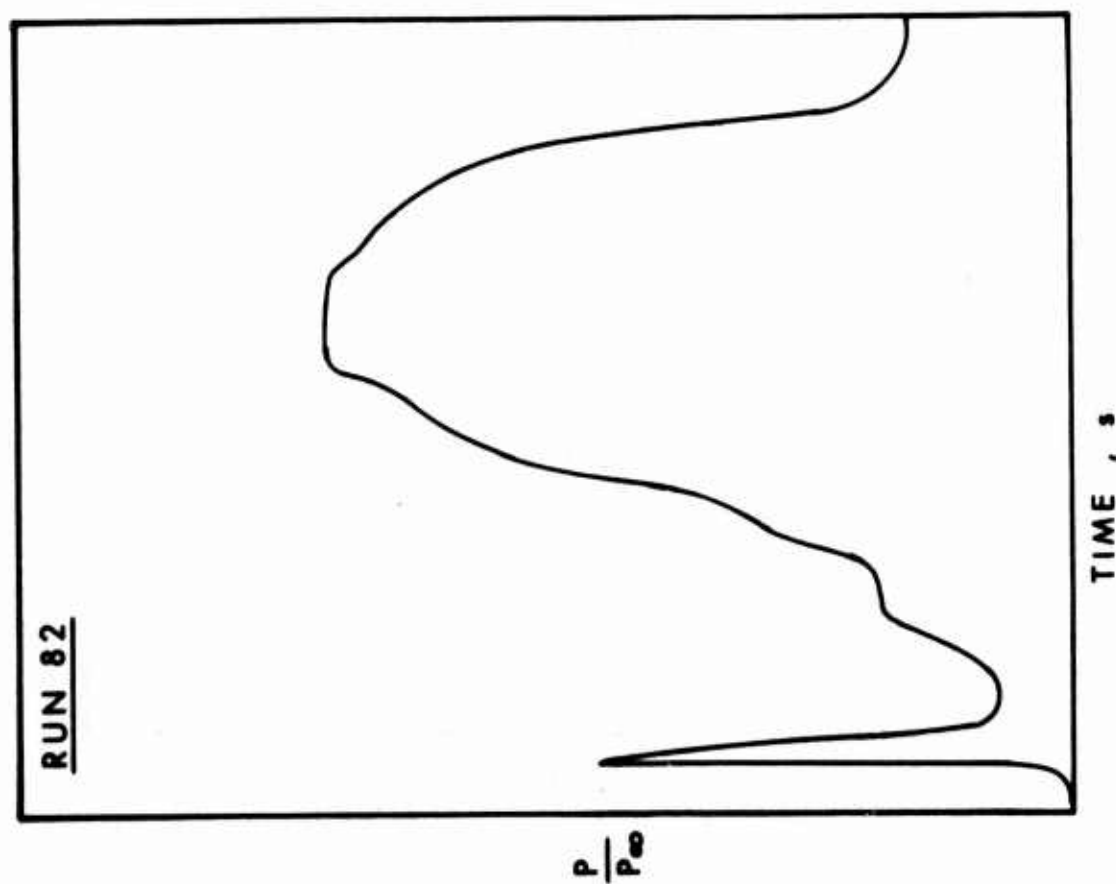
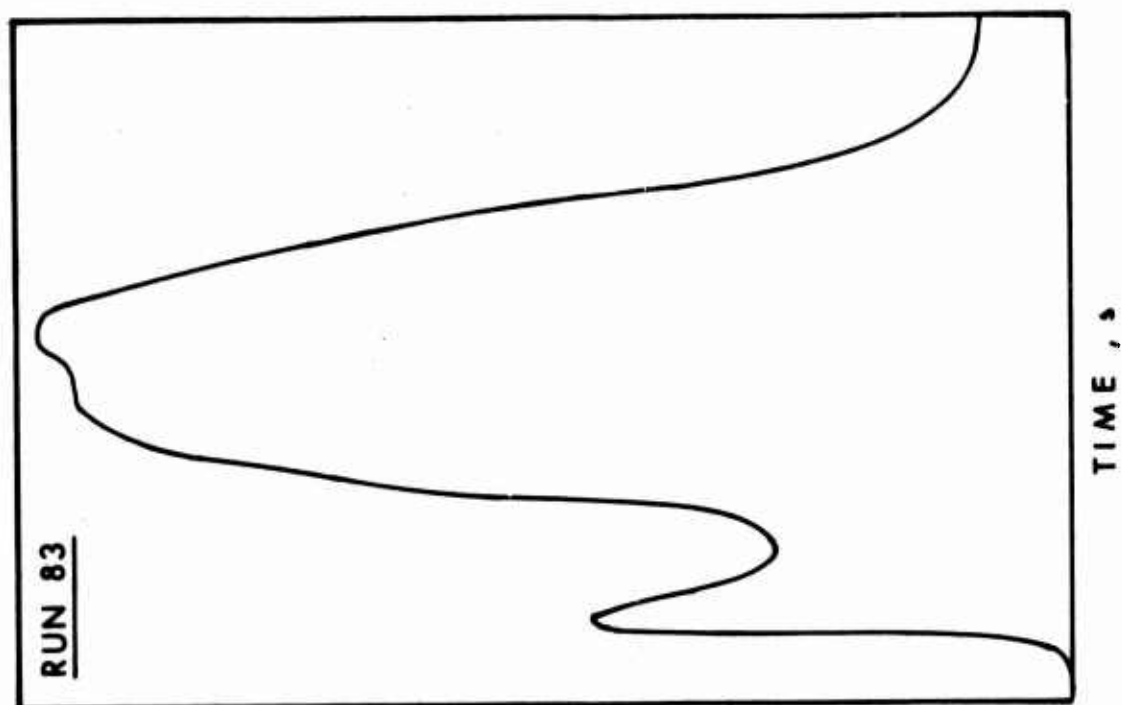


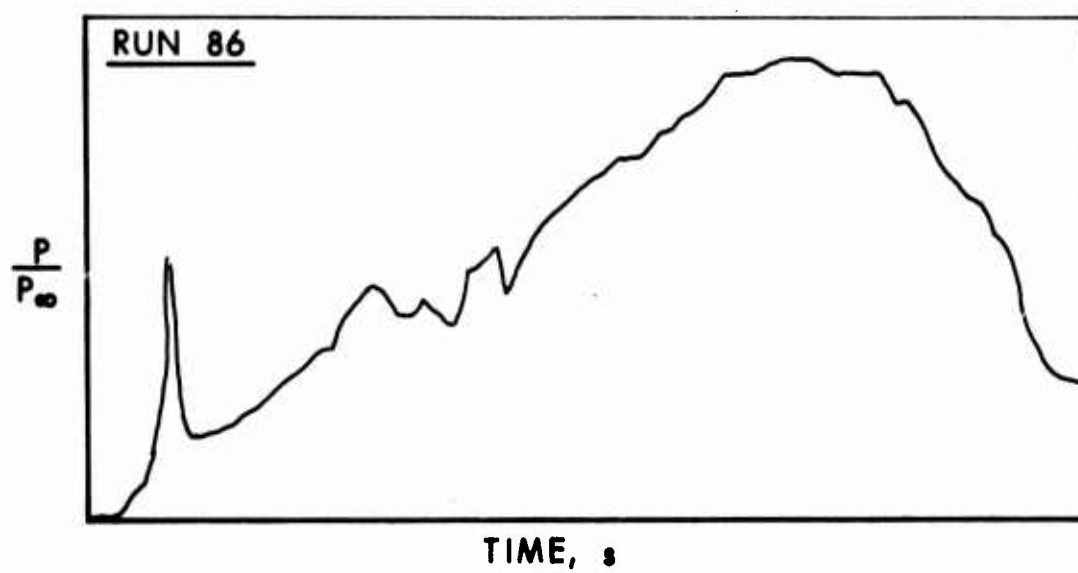
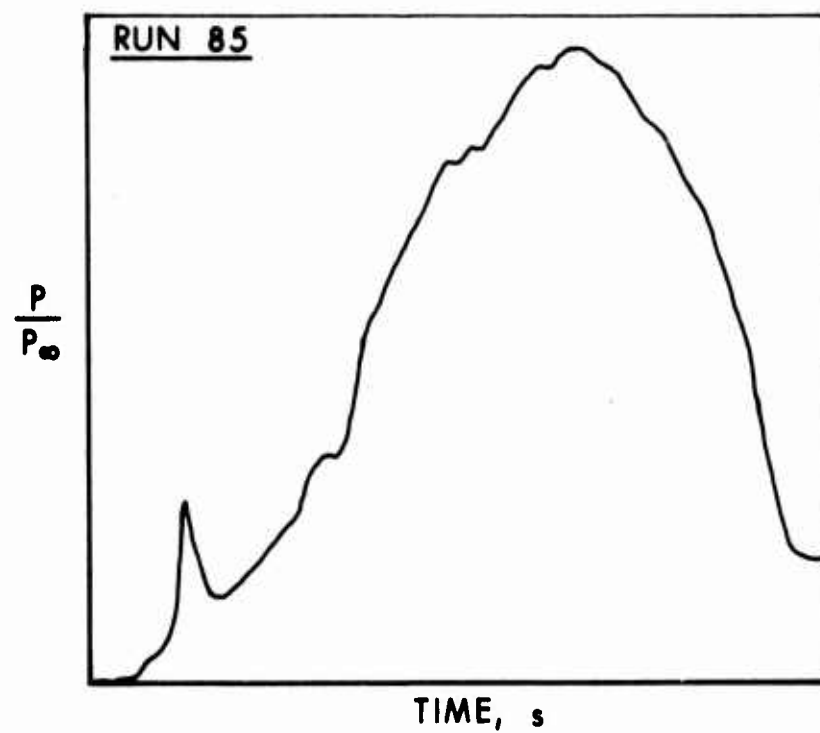


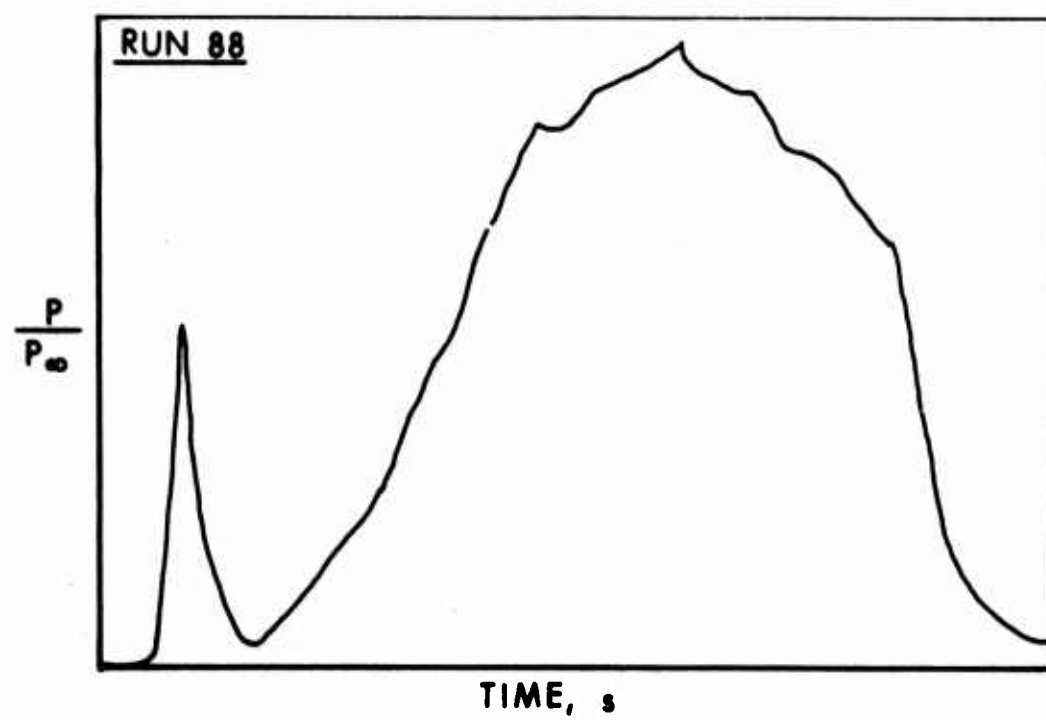
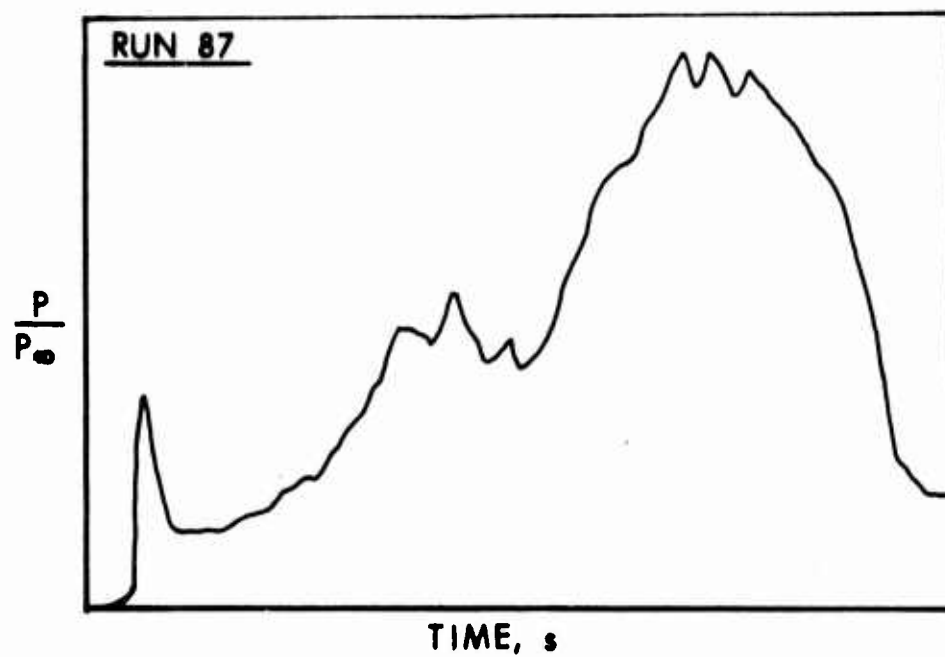


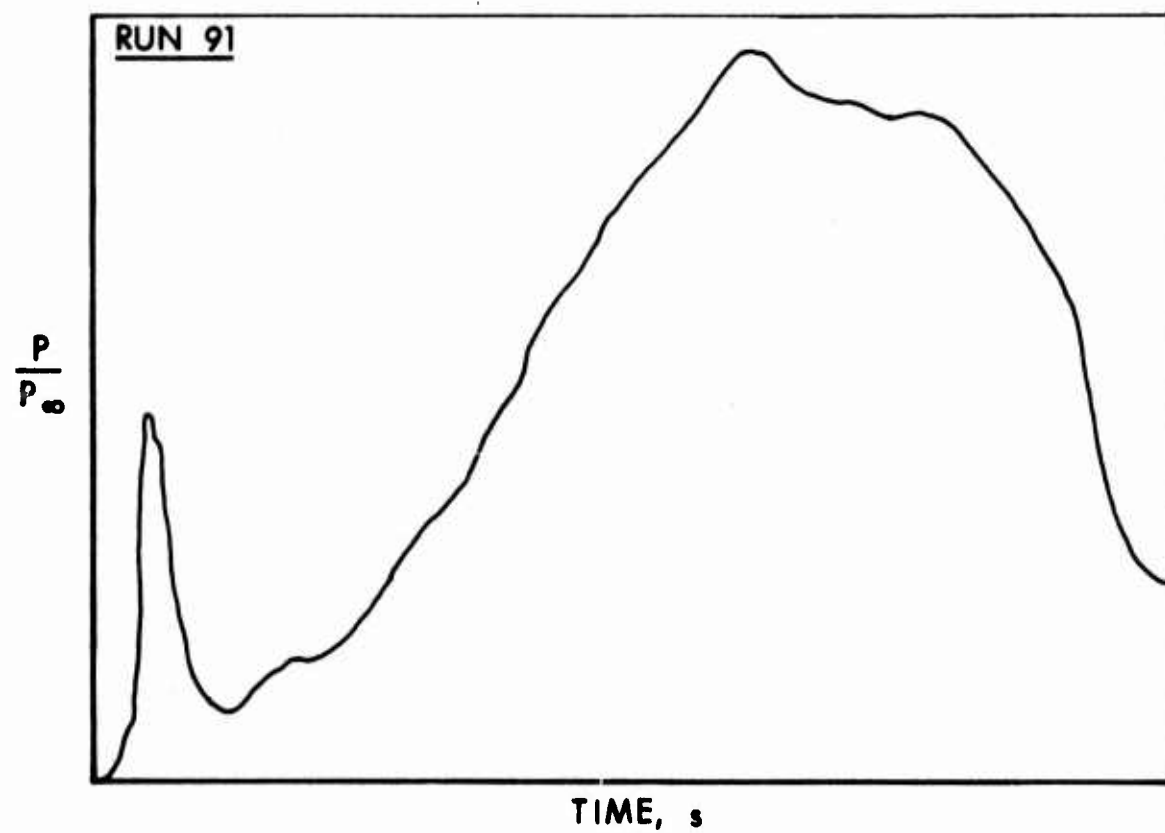
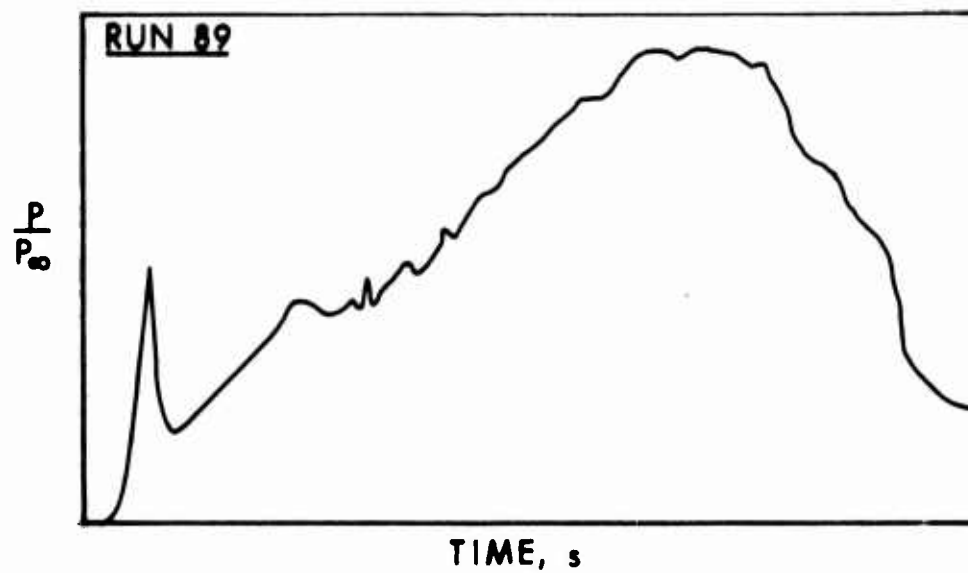


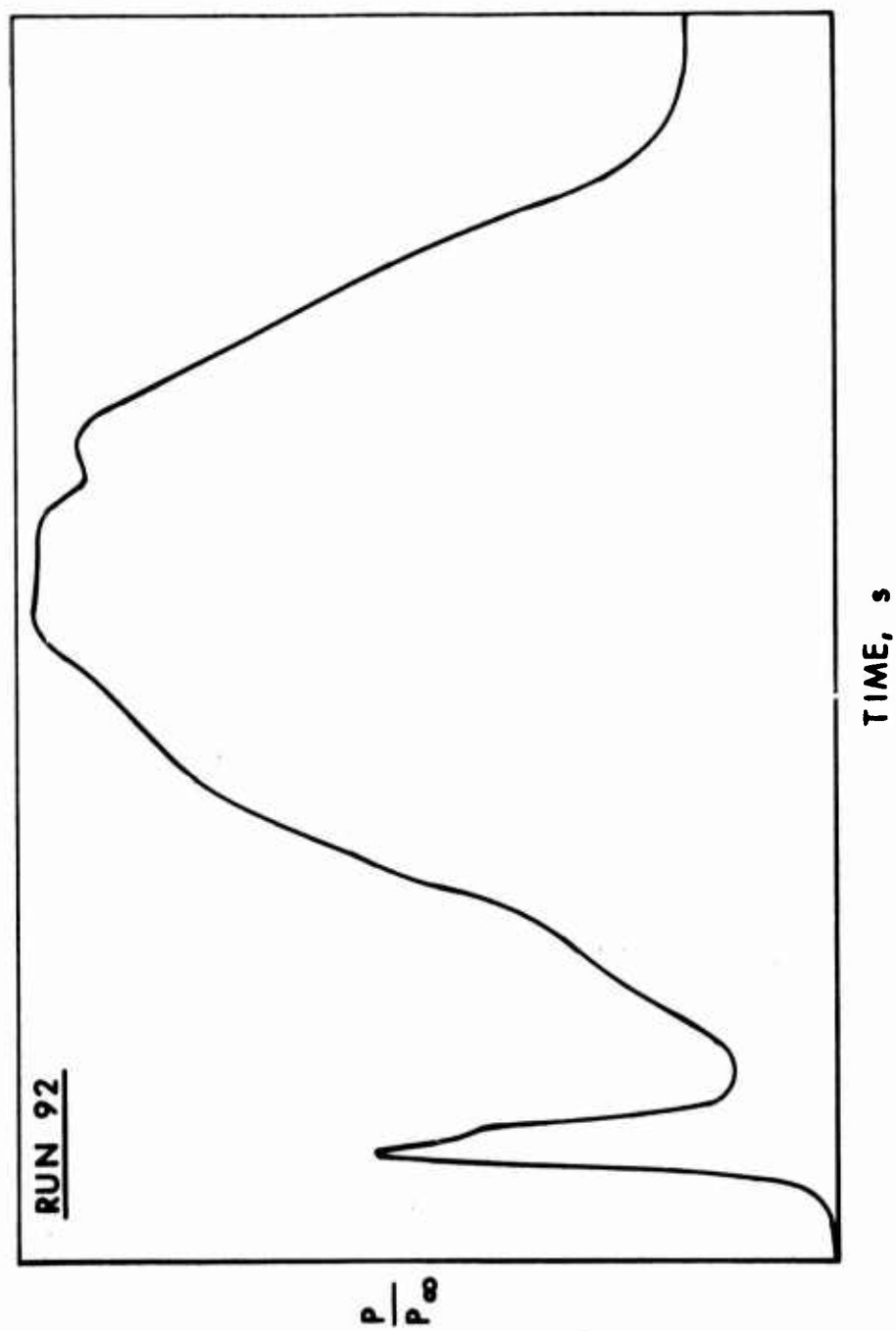


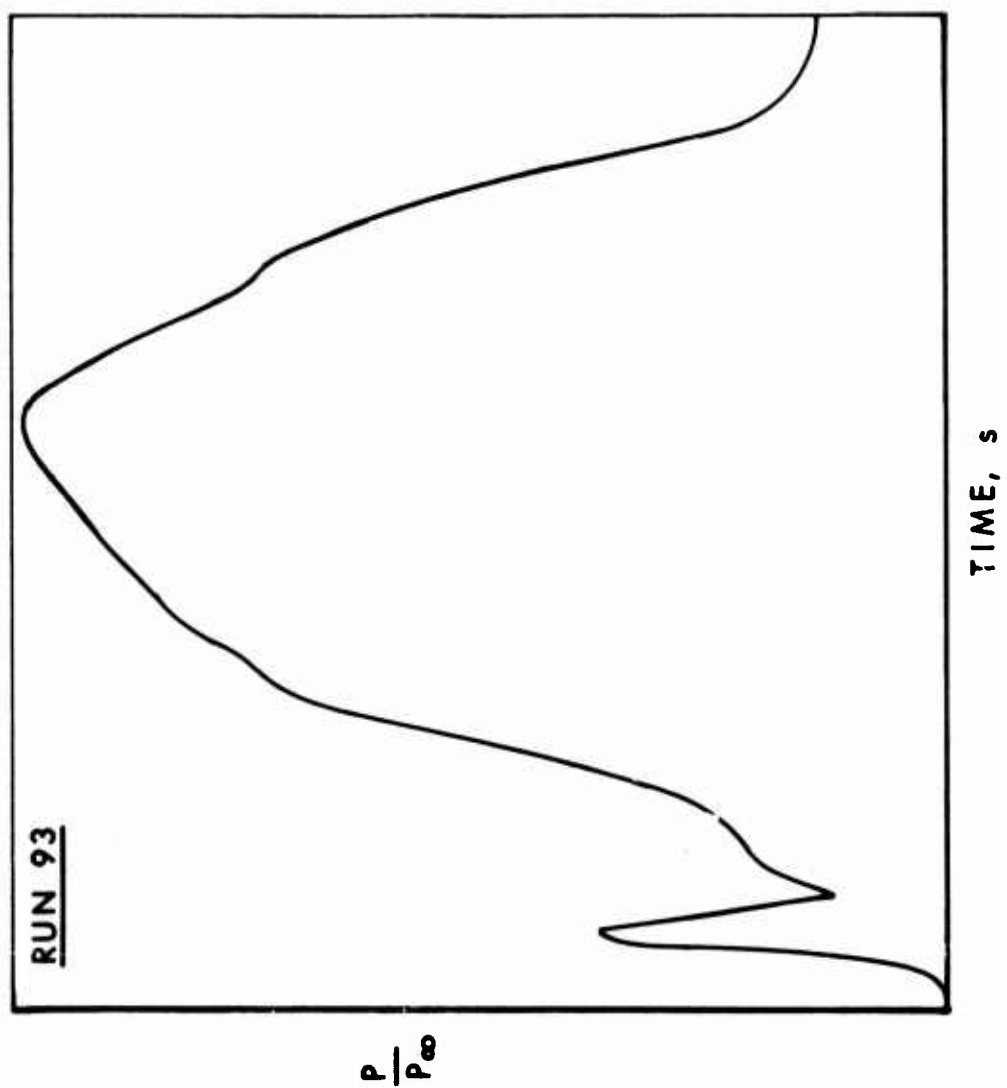


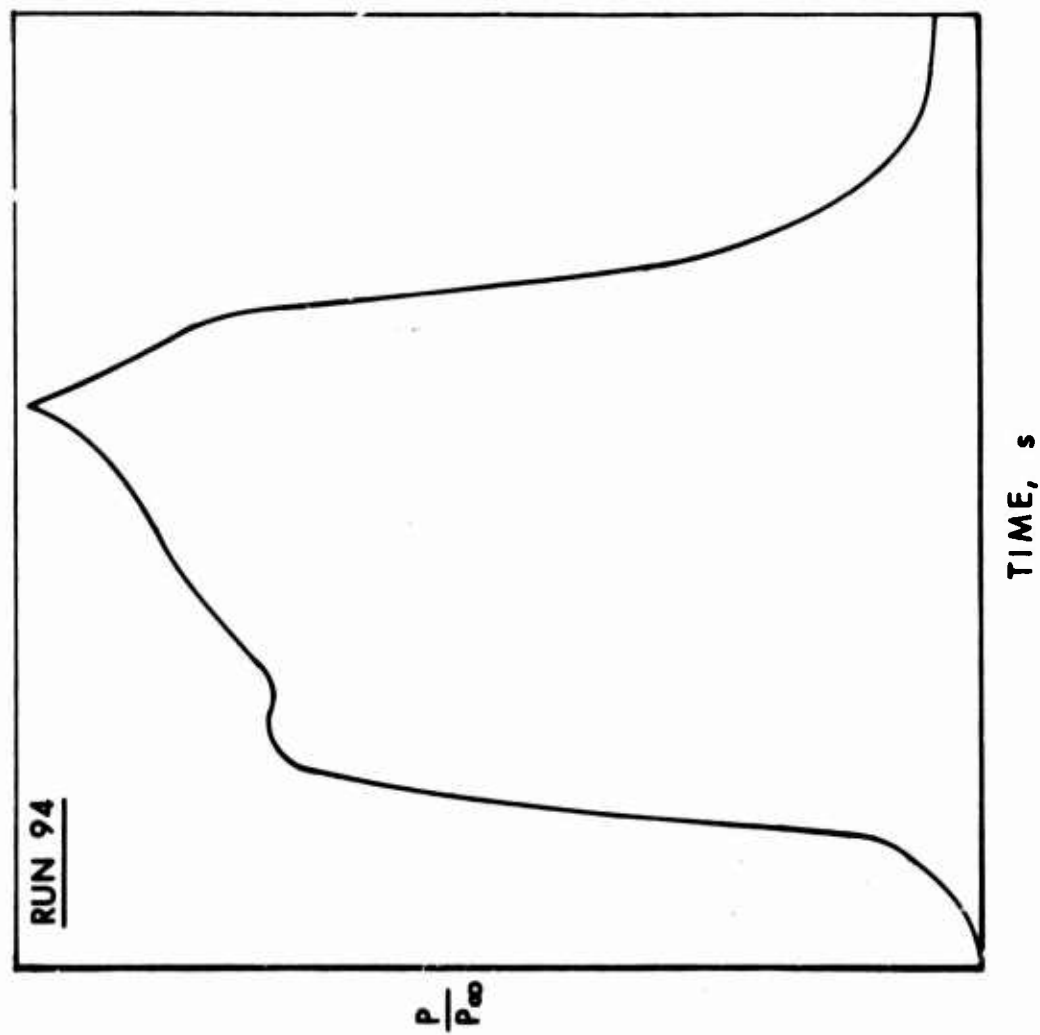












DISTRIBUTION LIST

<u>No. of</u> <u>Copies</u>	<u>Organization</u>	<u>No. of</u> <u>Copies</u>	<u>Organization</u>
2	Commander Defense Documentation Center ATTN: DDC-TCA Cameron Station Alexandria, VA 22314	1	Commander US Army Tank Automotive Development Command ATTN: DRDTA-RWL Warren, MI 48090
1	Director Institute for Defense Analysis ATTN: Dr. H. Wolfhard 400 Army Navy Drive Arlington, VA 22202	2	Commander US Army Mobility Equipment Research & Development Command ATTN: Tech Docu Cen, Bldg. 315 DRSME-RZT Fort Belvoir, VA 22060
1	Commander US Army Materiel Development and Readiness Command ATTN: DRCDMA-ST 5001 Eisenhower Avenue Alexandria, VA 22333	1	Commander US Army Armament Materiel Readiness Command Rock Island, IL 61202
1	Commander US Army Aviation Systems Command ATTN: DRS-AV-E 12th and Spruce Streets St. Louis, MO 63166	4	Commander US Army Armament Research and Development Command ATTN: DRDAR-LC, H. Hudgins D. Katz S. Kravitz A. LoPresti Dover, NJ 07801
1	Director US Army Air Mobility Research and Development Laboratory Ames Research Center Moffett Field, CA 94035	5	Commander US Army Armament Research and Development Command ATTN: DRDAR-LC, F. Taylor N. Weins D. Werbel R. Riesman A. Moss Dover, NJ 07801
1	Commander US Army Electronics Command ATTN: DRSEL-RD Fort Monmouth, NJ 07703		
4	Commander US Army Missile Command ATTN: DRDMI-R DRDMI-RK Dr. R. Rhoades Mr. N. White Redstone Arsenal, AL 35809	6	Commander US Army Frankford Arsenal ATTN: C. Dickey R. Kwatnoski T. Elmendorf G. Bornheim W. Gadowski D. Mancinelli Philadelphia, PA 19137

DISTRIBUTION LIST

<u>No. of Copies</u>	<u>Organization</u>	<u>No. of Copies</u>	<u>Organization</u>
1	Commander US Army White Sands Missile Range ATTN: STEWS-VT White Sands, NM 88002	3	Commander US Naval Ordnance Systems Command ATTN: ORD-0632 ORD-035 ORD-5524 Washington, DC 20360
1	Commander US Army Harry Diamond Labs ATTN: DRXDO-TI 2800 Powder Mill Road Adelphi, MD 20783	1	Chief of Naval Research ATTN: ONR-429 Department of the Navy Washington, DC 20360
1	Commander US Army Materials and Mechanics Research Center ATTN: DRXMR-ATL Watertown, MA 02172	1	Commander US Naval Missile Center ATTN: Code 5632 Point Mugu, CA 93041
1	Commander US Army Natick Research and Development Command ATTN: DRXRE, Dr. D. Sieling Natick, MA 01762	1	Commander US Naval Surface Weapons Center ATTN: Tech Lib Dahlgren, VA 22448
1	Director US Army TRADOC Systems Analysis Activity ATTN: ATAA-SA White Sands, NM 88002	4	Commander US Naval Surface Weapons Center ATTN: Code 730 F. Baltakis S. Hastings F. Moore Silver Springs, MD 20910
2	Commander US Army Research Office ATTN: Mr. R. Heaston Tech Lib P. O. Box 12211 Research Triangle Park NC 27709	3	Commander US Naval Weapons Center ATTN: Code 608 Dr. J. Prentice Code 753, Tech Lib Dr. K. Schadow China Lake, CA 93555
3	Commander US Naval Air Systems Command ATTN: AIR-604 Washington, DC 20360	2	Commander US Naval Ammunition Depot ATTN: B. Douda J. Tanner Crane, IN 47522

DISTRIBUTION LIST

<u>No. of</u> <u>Copies</u>	<u>Organization</u>	<u>No. of</u> <u>Copies</u>	<u>Organization</u>
1	Commander US Naval Research Laboratory ATTN: Code 6180 Washington, DC 20375	1	Director National Aeronautics and Space Administration John F. Kennedy Space Center ATTN: KSC Lib - NWSI-D Kennedy Space Center, FL 32899
2	Superintendent US Naval Postgraduate School ATTN: Tech Lib A. Fuhs Indian Head, MD 20640	1	Director National Aeronautics and Space Administration Langley Research Center ATTN: MS-185, Tech Lib Langley Station Hampton, VA 23365
1	AFSC (DOL) Andrews AFB Washington, DC 20331	2	Director National Aeronautics and Space Administration ATTN: MS-603, Tech Lib MS-86, Dr. Povinelli 21000 Brookpark Road Lewis Research Center Cleveland, OH 44135
1	AFOSR (SREP) Bolling AFB, DC 20332	1	Director National Aeronautics and Space Administration Manned Spacecraft Center ATTN: Tech Lib Houston, TX 77058
2	AFRPL (RPMCP, Dr. R. Weiss; Dr. R. Schoner) Edwards AFB, CA 93523	1	Aerojet Solid Propulsion Co ATTN: Dr. P. Micheli Sacramento, CA 95813
2	Headquarters National Aeronautics and Space Administration ATTN: RPS; RP Washington, DC 20546	1	ARO Incorporated ATTN: Mr. N. Dougherty Arnold AFS, TN 37389
1	Director National Aeronautics and Space Administration George C. Marshall Space Flight Center ATTN: Tech Lib Huntsville, AL 35812	1	Atlantic Research Corporation ATTN: Tech Lib Shirley Highway at Edsall Road Alexandria, VA 22314
1	Director Jet Propulsion Laboratory ATTN: Tech Lib 4800 Oak Grove Drive Pasadena, CA 91103		

DISTRIBUTION LIST

<u>No. of</u> <u>Copies</u>	<u>Organization</u>	<u>No. of</u> <u>Copies</u>	<u>Organization</u>
1	Calspan Corporation P. O. Box 235 Buffalo, NY 14221	1	The Marquardt Corporation ATTN: Tech Lib P. O. Box 2013 Van Nuys, CA 91404
1	Dow Chemical Company ATTN: George Lane Midland, MI 48640	1	The Martin-Marietta Corporation Denver Division ATTN: Res Lib P. O. Box 179 Denver, CO 80201
1	Explosives Corp of America ATTN: Patrick A. Yates P.O. Box 906 Redmond, WA 98052	1	MB Associates ATTN: Dr. A. McCone San Ramone, CA 94583
1	General Electric Company Flight Propulsion Division ATTN: Tech Lib Cincinnati, OH 45215	2	North American Rockwell Corp Rocketdyne Division ATTN: Dr. C. Oberg Tech Lib 6633 Canoga Avenue Canoga Park, CA 91304
2	Hercules Incorporated Alleghany Ballistic Labs ATTN: Dr. R. Yount Tech Lib Cumberland, MD 21501	2	North American Rockwell Corp Rocketdyne Division ATTN: Mr. W. Haymes Tech Lib McGregor, TX 76557
1	Hercules Incorporated Bacchus Division ATTN: Dr. M. Beckstead Magna, UT 84044	3	Thiokol Chemical Corporation Huntsville Division ATTN: Dr. D. Flanigan Tech Lib E. Barnes Huntsville, AL 35807
1	Lockheed Palo Alto Research Lab ATTN: Tech Info Center 3251 Hanover Street Palo Alto, CA 94304	1	Thiokol Chemical Corporation Longhorn Division ATTN: Dave Dillehay Marshall, TX 79843
1	Lockheed Propulsion Company ATTN: Dr. N. Cohen P. O. Box 111 Redlands, CA 92373	3	Thiokol Chemical Corporation Wasatch Division ATTN: Dr. M. Muhlfeith Graham Shaw Tech Lib P. O. Box 524 Brigham City, UT 84302
1	McDonnell Douglas Corporation Missile & Space Sys Div ATTN: Tech Lib Santa Monica, CA 90406		

DISTRIBUTION LIST

<u>No. of</u> <u>Copies</u>	<u>Organization</u>	<u>No. of</u> <u>Copies</u>	<u>Organization</u>
1	TRW Systems Group ATTN: Mr. H. Korman One Space Park Redondo Beach, CA 90278	3	Georgia Institute of Technology School of Aerospace Engineering ATTN: Prof. B. Zinn Prof. W. Strahle Prof. E. Price Atlanta, GA 30333
1	United Aircraft Corporation Pratt and Whitney Division ATTN: Tech Lib P. O. Box 2691 West Palm Beach, FL 33402	1	IIT Research Institute ATTN: Prof. T. Torda 10 West 35th Street Chicago, IL 60616
1	United Aircraft Corporation Research Laboratories ATTN: Dr. R. Waesche East Hartford, CT 06108	2	Director Chemical Propulsion Information Agency The Johns Hopkins University ATTN: Mr. T. Christian Tech Lib Johns Hopkins Road Laurel, MD 20810
2	United Technology Center ATTN: Dr. R. Brown Tech Lib P. O. Box 358 Sunnyvale, CA 94088	1	Massachusetts Institute of Technology Dept of Mechanical Engineering ATTN: Prof. G. Faeth University Park, PA 16802
1	Battelle Memorial Institute ATTN: Tech Lib 505 King Avenue Columbus, OH 43201	2	Princeton University Dept of Aerospace and Mechanical Sciences ATTN: Prof. I. Glassman Tech Lib James Forrestal Campus Princeton, NJ 08540
2	Brigham Young University Dept of Chemical Engineering ATTN: Prof. R. Coates Prof. M. Horton Provo, UT 84601	1	Forrestal Campus Library Princeton University ATTN: Prof. M. Summerfield P. O. Box 710 Princeton, NJ 08540
2	California Institute of Tech ATTN: Prof. F. Culick Tech Lib 1201 East California Boulevard Pasadena, CA 91102		
1	Case Western Reserve University Division of Aerospace Sciences ATTN: Prof. J. Tien Cleveland, OH 44135		

DISTRIBUTION LIST

<u>No. of</u> <u>Copies</u>	<u>Organization</u>	<u>No. of</u> <u>Copies</u>	<u>Organization</u>
7	Purdue University School of Mechanical Engineering ATTN: Prof F. Osborn Prof S. N. B. Murthy John Andrews Duane Baker Prof B. A. Reese Harry Bruestle Prof D. E. Abbott Lafayette, IN 47907	2	University of Illinois Dept of Aeronautical Engineering ATTN: Prof H. Krier Prof R. Strehlow Urbana, IL 61803
1	Rutgers-State University Dept of Mechanical and Aerospace Engineering ATTN: Prof S. Temkin University Heights Campus New Brunswick, NJ 08903	1	University of Minnesota Dept of Mechanical Engineering ATTN: Prof E. Fletcher Minneapolis, MN 55455
1	Stanford Research Institute Propulsion Sciences Division ATTN: Tech Lib 333 Ravenswood Avenue Menlo Park, CA 94204	2	University of Utah Dept of Chemical Engineering ATTN: Prof A. Baer Prof G. Flandro Salt Lake City, UT 84112
1	Stevens Institute of Technology Davidson Laboratory ATTN: Prof R. McAlevy III Hoboken, NJ 07030		<u>Aberdeen Proving Ground</u> Marine Corps LnO Dir, USAMSAA
2	University of California Dept of Aerospace Engineering ATTN: Prof S. Penner Prof F. Williams La Jolla, CA 92037		
2	University of Denver Denver Research Institute ATTN: R. M. Blunt Tech Lib P. O. Box 10127 Denver, CO 80210		